2017

POLYMER WAVEGUIDE MANUFACTURING AND PRINTED CIRCUIT BOARD INTEGRATION

Brandon Swatowski
Michigan Technological University, bwswatow@mtu.edu

POLYMER WAVEGUIDE MANUFACTURING AND PRINTED CIRCUIT BOARD INTEGRATION

By

Brandon William Swatowski

A THESIS

Submitted in partial fulfillment of the requirements for the degree of

MASTER OF SCIENCE

In Electrical Engineering

MICHIGAN TECHNOLOGICAL UNIVERSITY

2017

This thesis has been approved in partial fulfillment of the requirements for the Degree of MASTER OF SCIENCE in Electrical Engineering.

Department of Electrical Engineering

Thesis Advisor:	*Dr. Christopher Middlebrook*
Committee Member:	*Dr. Michael Roggemann*
Committee Member:	*Dr. Paul Bergstrom*
Committee Member:	*Dr Craig Friedrich*
Department Chair:	*Dr. Daniel Furhmann*

Table of Contents

List of figures

List of tables

Acknowledgements

I would like to thank Dr. Christopher T. Middlebrook for guiding me during my time as a graduate student.

I would like to thank my father John and mother Nancy for their love and support as well as my wife Nichole for her understanding.

I would like to extend my gratitude to Dow Corning for allowing me to perform this research and for their materials and expertise.

Abstract

In this age of ever increasing data rates in communication systems, optics are becoming more commonplace for long length (>10m) signal transmission in High Performance Computing (HPC) systems due to their bandwidth capabilities which are higher than their electrical counterparts. In these optical based communication systems, Vertical Cavity Surface Emitting Lasers (VCSELs) are the most commonly used communications lasing medium for multimode fiber applications. These lasers are active in the 850 nm region, with speeds commonly at 10 Gbps/channel. VCSEL vendors are now commercializing lasers at 25 Gbps/channel as well, with research groups actively pursuing rates beyond 40 Gbps/channel, demonstrating that these communications technologies will likely be continuously incorporated in multiple generations of HPC systems.

For optical based signaling technologies, fiber optics are typically utilized as the medium of choice for point to point contacts due to their low loss characteristics, stability to thermal degradation and aging, and manufacturability. Fiber optics have become a commodity, making them inexpensive. However, the high precision connection technologies required to bring light off of VSCELS and fiber to fiber are still rather expensive, limiting some of the optical applications in products. Polymer waveguides offer the promise to act as an enabling technology to provide highly complex optical routing that can be passively connected, lowering system costs and allowing next generation systems to be optically driven. For this to become a reality, polymer waveguide materials must meet multiple requirements in the communications industry.

The focus of this thesis is on the understanding and optimization of the manufacturing requirements of polymer waveguide materials, their optical stability to existing standards such as Telecordia, and the impacts that printed circuit board processes have on them.

1 Introduction

Over the last decade, the continuous demand for greater speed and lower energy consumption in high bandwidth data links has driven the adoption of optical signaling in server backplanes due to the inherent limitations of copper technologies. As data rates continue to increase for consumer markets such as mobile communications, internet, and streaming media, data centers have increased their bandwidth capacities by a factor of 10 every 4 years and can be seen in Figure 1. To increase this bandwidth, copper based signaling technologies are dominantly utilized with each technological node increasing in design complexity and cost [1-4].

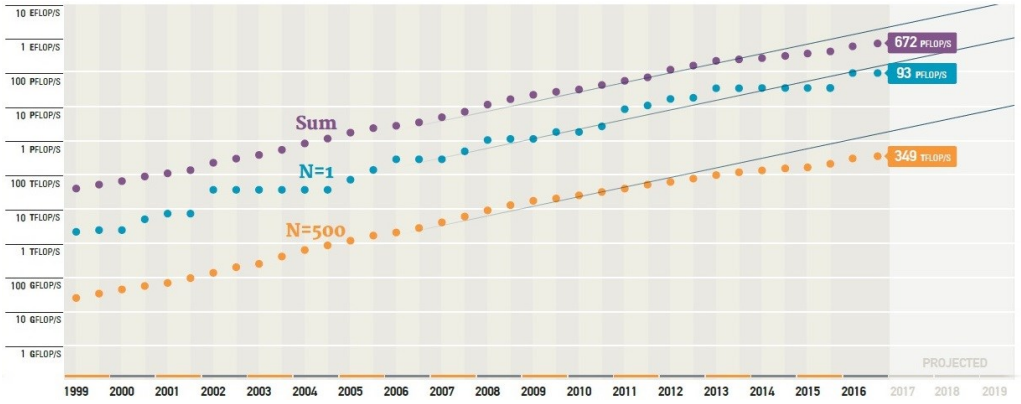

Figure 1: Project Data Rate Growth of Top 500 Super Computers [5]

Optical based technologies utilizing fiber optical connections are now more commonly being utilized to alleviate the issues with electrical based signaling at higher data rates [6-11]. However, these advances introduce manufacturing and density problems as fiber optical connections are not pre-routed connections like their electrical counterparts

(Figure 2). The development of a method to route these optical connections in a cost effective manner is required to continue growth of optical based signaling technologies.

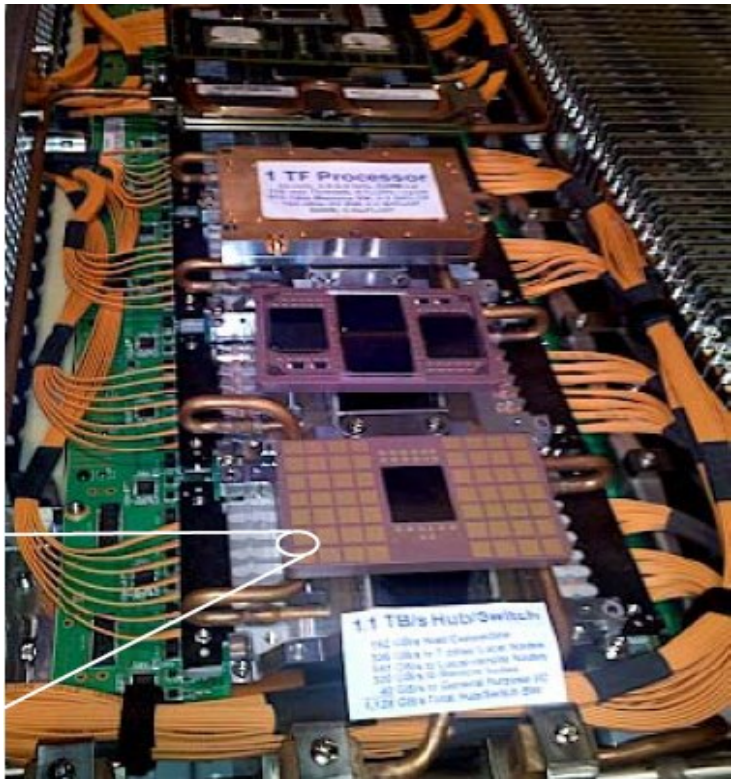

Figure 2: Blue Waters Line Card Demonstrating Fiber Connections [12]

Polymer waveguides serve as a potential candidate to enable high-density optical interconnections in data center architectures [13-18]. Polymer waveguides typically are photopatternable materials that can be manufactured into complex optical routings (Figure 3) on a small form factor (Figure 4). These materials can be manufactured onto flexible optical backplane (Figure 4) or embedded into printed circuit boards (Figure 5).

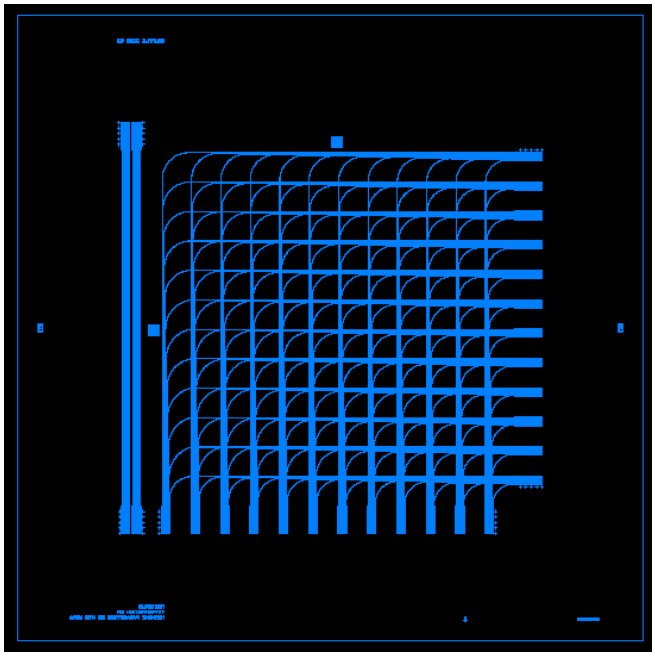

Figure 3: 12x12 Optical Shuffle Mask for Polymer Waveguide Manufacturing

Figure 4: Polymer Waveguide Flex Ribbon Consisting of 8 Polymer Waveguide Layers[19]

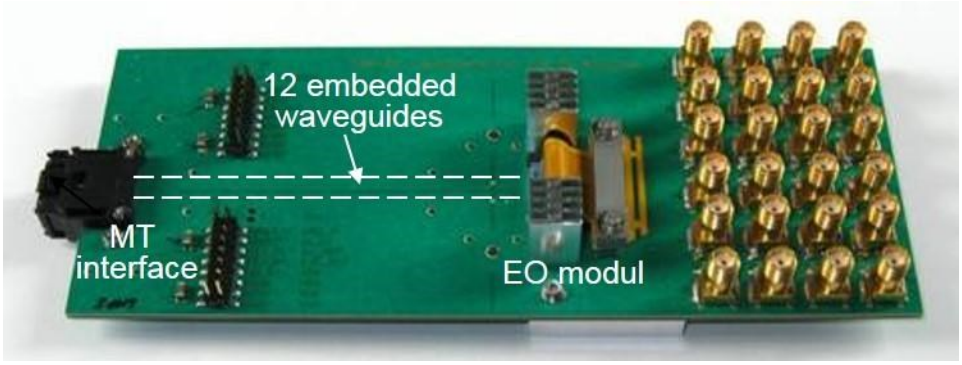

Figure 5: Embedded Polymer Waveguides in Printed Circuit Board [20]

For polymer waveguides to become a realistic technology for optical signal routing, manufacturing and stability requirements of the existing optical and printed circuit board industry must be maintained [21-23]. The layout of this Thesis is as follows; first, the theoretical foundations of optical propagation will be detailed, along with the measurement techniques associated with the optical analyses presented in this document. Second, the optimization process of polymer waveguide manufacturing and their corresponding optical stability determined through Telecordia testing will be examined. Last, the process used to manufacture printed circuit boards, and the impacts this manufacturing process has on the optical performance of polymer waveguides will be examined.

2 Optical Propagation

When light travels from a high index material into a low index material, a portion of the light is reflected and a portion is transmitted. The transmitted light enters the low RI medium at an angle that is calculated through the relationship in Equation 2.1 known as Snell's Law of Refraction (Figure 6).

Equation 1

$$n_1 sin\ \theta_1 = n_2 sin\ \theta_2$$

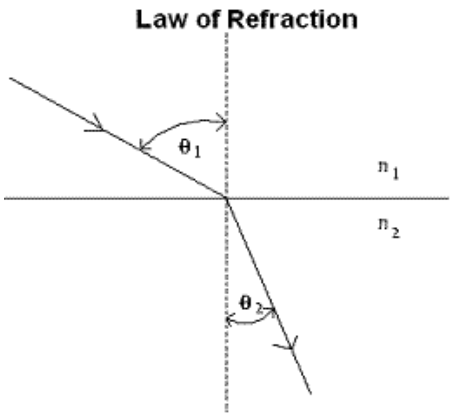

Figure 6: Snell's' Law of Refraction

When the angle of the high index material is large enough, the angle of refraction into the low index material is 90° as can be seen in Equation 2 and Figure 7. At this critical angle, all light is being reflected back into the high index material so no light is being transmitted into the low index material. This is referred to as total internal reflection. This fundamental optical property of materials allows fiber optic propagation to occur.

Equation 2

$$\theta_1 \geq sin^{-1}\ \frac{n_1}{n_2}$$

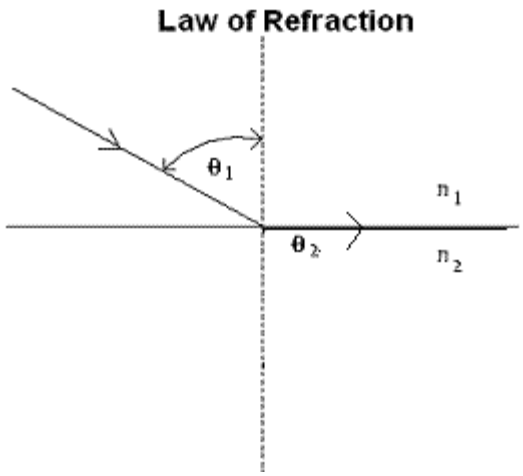

Figure 7: Total Internal Reflection

2.1 Propagation of Optical Signals

Applying Snell's law of refraction between two interfaces and further extending it to a 2 dimensional rectangular slab with $n_1 > n_2$ (Figure 8), one can calculate the requirements of n1, n2, and θ_1 restrict light to transmitting through a high index medium with no losses due to refraction. Taking Equation 3-5, θ_1 can be solved in terms of n_1 and n_2. Equation 6 is the resulting relationship between the three variables and it can be seen that the angle of light entering a slab waveguide following the TIR principle is dependent on only the refractive indices of the two materials. This value is defined as the numerical aperture (NA) which is a measure of what angles of light are accepted into the waveguide and propagate without any refractive losses. When utilized in a wave guiding system these materials are known as a core and clad where the core is the high RI region and the cladding is the low RI region.

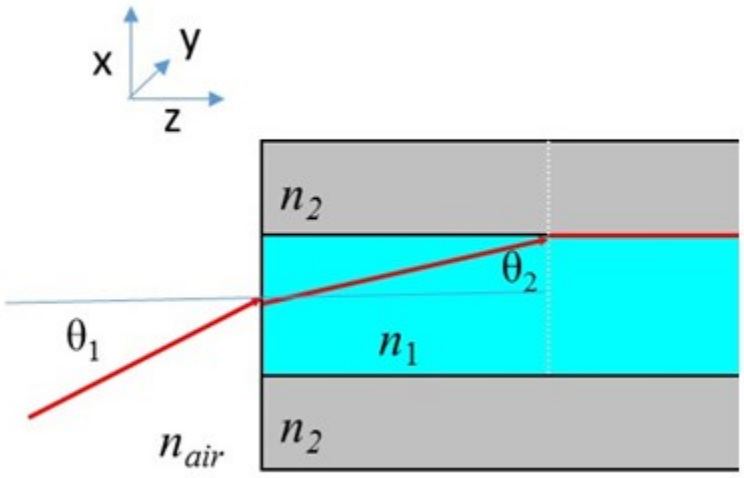

Figure 8: Slab Waveguide

Equation 3

$$n_{air} sin\ \theta_1 = n_1 sin\ \theta_2$$

Equation 4

$$n_1 sin\ (90 - \theta_2) \geq n_2 sin\ 90$$

Equation 5

$$cos^2\ \theta_2 + sin^2\ \theta_2 = 1$$

Equation 6

$$NA \equiv sin\ \theta_1 \leq \sqrt{n_1^2 - n_2^2}$$

Extending this optical phenomenon to 3 dimensions, Figure 9 depicts optical signaling being sent down a fiber optic. These optical fiber signals totally internally reflect, transmitting down the axis of a fiber optic to its source destination. The level of the signal received is determined by two properties of the fiber optic, the attenuation and dispersion. Attenuation, is the optical power loss of a fiber due to absorptions and scattering in the fiber. Dispersion is the amount that a signal will spread over a distance and is dependent on multiple factors such as fiber size, shape, NA, and others.

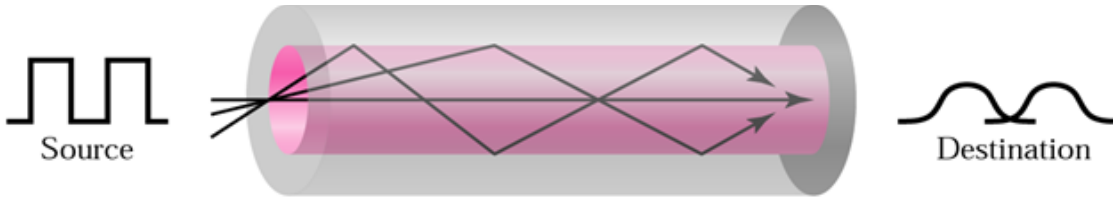

Figure 9: Fiber Optic Propagation

Attenuation is defined as the exponential loss of light in a medium due to its intrinsic and extrinsic properties [24]. For optical fibers and waveguides, the majority of attenuation is attributed to the material's molecular absorption of light and scattering due to impurities in the material or other optical phenomenon such as Rayleigh scattering. Attenuation is one of the primary factors in determining optical link lengths and viability in utilization of an optical channel. Figure 10 shows the optical absorption spectrum of a fiber optic, demonstrating an optical absorption of ~3-4 dB/km at the wavelength of interest 850 nm. These losses are very low for commercially available materials. Subsequently, this is the primary reason glass is utilized for the majority of optical communications across distances. For polymers, optical absorption is much higher due to molecular absorption and higher scattering losses, on the order of 3-4 dB/m (Figure 11). For this reason, polymer waveguides are not suitable for long range applications (>5m) and the technical focus is on printed circuit board applications where link lengths are less than 2 m. Due to the significant importance that attenuation plays on the viability of optical signaling, the majority of this thesis focuses on the attenuation loss of polymer waveguide devices and the extrinsic impacts that manufacturing and outside degradations have on signal performance.

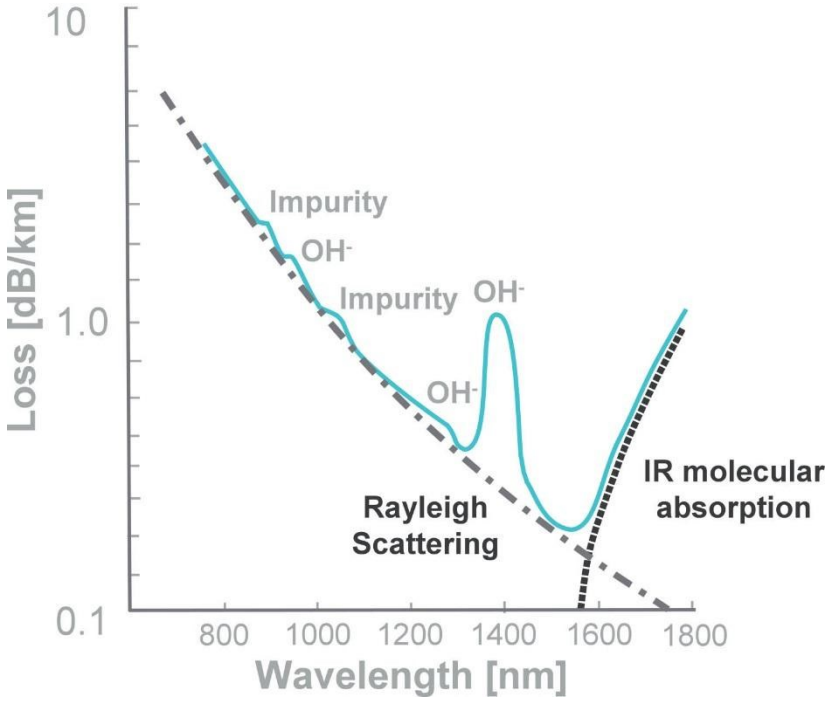

Figure 10: Optical fiber absorption spectrum [26]

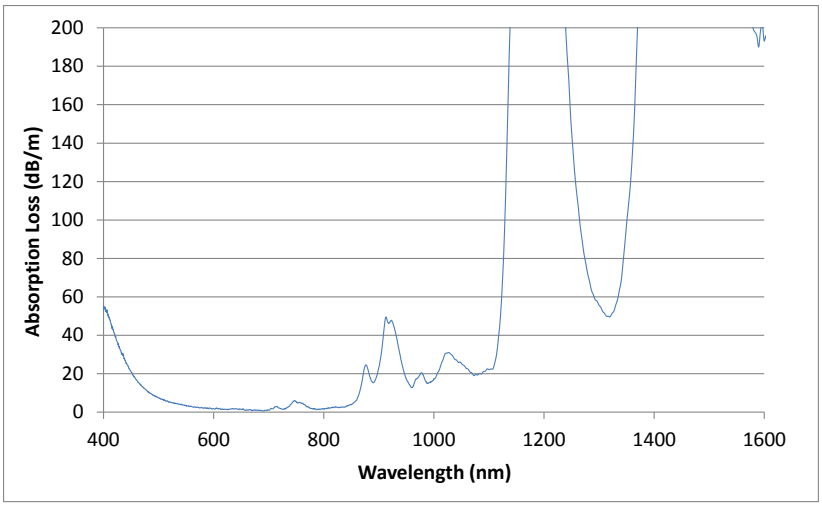

Figure 11: Optical attenuation of polymer waveguide

Optical dispersion is a measure of the pulse broadening of a signal in an optical channel over a distance [27]. This occurs due to multiple factors. First, light can travel down multiple paths while traveling down a fiber and this results in different total path lengths and pulse broadening. This is an example of modal dispersion and is dependent on device properties such as waveguide size and the refractive index difference between core and clad. For multimode fibers and waveguides, modal dispersion is the primary cause of dispersion. The other major cause of dispersion is chromatic dispersion; Chromatic dispersion occurs because the speed of light in a medium is different for different wavelengths and since optical sources have a finite spectral output, the different wavelengths of light travel at different speeds[27]. Chromatic dispersion is a major factor in the manufacture of single mode fibers where there is only one path for light and modal dispersion does not have an impact. For multimode links, chromatic dispersion has only a small impact compared to modal dispersion and is typically ignored. Overall, dispersion plays an important role in optical communications especially over long distances (>1 km), but in the scope of this document, links of 2 m or less do not suffer significantly from dispersion so they have not been analyzed in detail.

3 Fabrication, Testing, and Measurement of Polymer Waveguides

Multiple methods exist to manufacture, prepare, and test polymer waveguides to understand their optical propagation properties. Although all of these methods are not discussed in this thesis, there are multiple references to such methods [13-14]. This section focuses on how the polymer waveguides discussed in this thesis are fabricated, prepared, and tested.

3.1 Fabrication

The material used in this research are a liquid photo definable polymer material. The methodology to fabricate polymer waveguides with these materials is a layered deposition approach in which the liquid material is first applied, then the solvent it contains is removed via a thermal step (soft bake). The material is then polymerized with a UV cure step and finalized with a post exposure thermal step (hard bake). The core layer has an added step of solvent development to remove any core that is not included in the photopatterning step. This is done for all three layers of material and a process flow diagram can be seen in Figure 12.

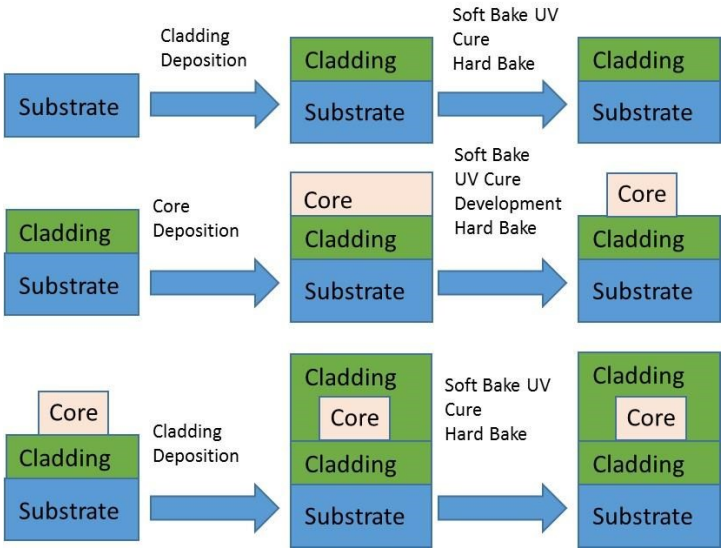

Figure 12: PWG Process Flow Diagram

After the polymer waveguides have been fabricated, they are separated using a diamond dicing saw. Saw marks from the diamond dicing saw on the waveguide endfaces can cause variations in the optical measurements so optical polishing techniques are employed to increase coupling efficiency and ensure homogeneity between each waveguide endface. A figure 8 pattern is applied to the waveguides on sand paper with grit sizes decreasing from 5 µm to 3 µm and lastly 1µm and then optically inspected. After the waveguide endfaces have been polished the entire substrate is cleaned with

isopropyl alcohol (IPA). Index matching fluid (1.45<n<1.52) is then applied to the ends of the substrate to minimize reflection losses between the fiber and waveguide (Figure 13).

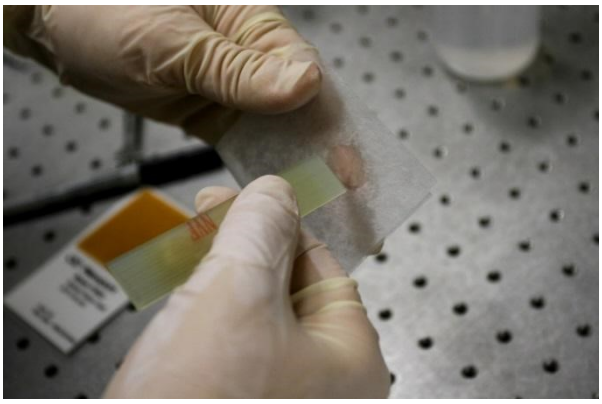

Figure 13: Application of Index Matching Fluid

The primary measurement used to inspect the optical properties of polymer waveguides is insertion loss which is defined as the logarithmic loss in signal power resulting from a transmission line system[25]. Mathematically, insertion loss can be seen as $IL = P_T - P_R$, where P_T and P_R are the transmitted and received power measured in dBm. Assuming the losses to be linear across the entire system, the loss per unit length or attenuation can be estimated by dividing by the length of the optical transmission line X and can be seen in Equation 7 .

Equation 7

$$L(\frac{dB}{cm}) = \frac{(P_T - P_R)}{X}$$

When measuring the insertion loss of polymer waveguides, direct coupling is used due to its simplicity and repeatability. Direct coupling involves using a laser source coupled to a single mode or multimode fiber that is used as the source of the system. This fiber input is then directly brought to the face of the waveguide to insert as much light as possible without the use of additional components. The light that propagates through the device under test is then received with a matched or oversized fiber to measure the overall system power loss. The schematic can be seen in Figure 14.

Figure 14: Direct Coupling Schematic

To perform the micromanipulation necessary for direct coupling, two Newport xyz stages with sub-micron resolution were used (Figure 15). A 5.7 µm 0.14 NA single mode fiber

operating at 830 nm was used as the input and a 50 μm 0.27 NA multimode fiber acted as the receiver for the light transferred through the waveguide. The optical power receivers used were Thorlabs standard silicon power sensors.

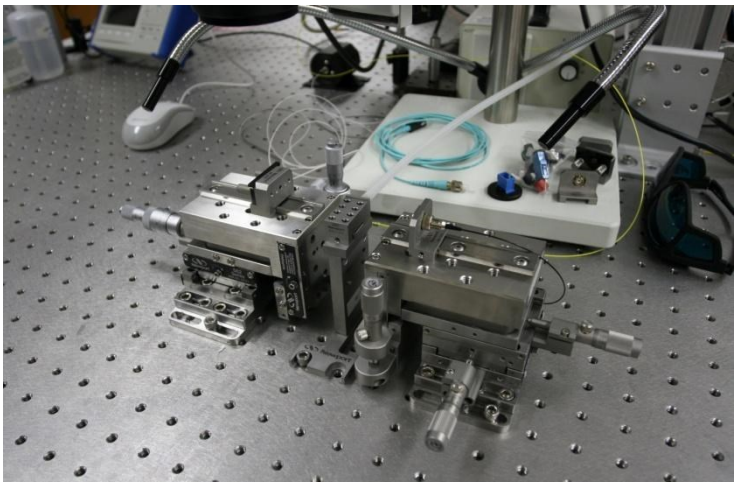

Figure 15: Direct Coupling Setup

To directly couple light to the waveguide the receiver is first removed and the input fiber is brought close to the waveguide substrate. Micromanipulation is performed to move the input fiber to the height of the waveguide core and cladding layer. In plane manipulation of the fiber allows transition between waveguides and the cladding layer between them. Coupling to a waveguide core is confirmed by using an infrared card to view light propagation through the optical material. Propagation through the waveguide core is rectangular in shape with a low amount of spreading of the beam as can be seen in Figure 16. Light propagation through the cladding layer between waveguides is elliptical in shape, corresponding to the spreading of the light in the cladding layer (Figure 17).

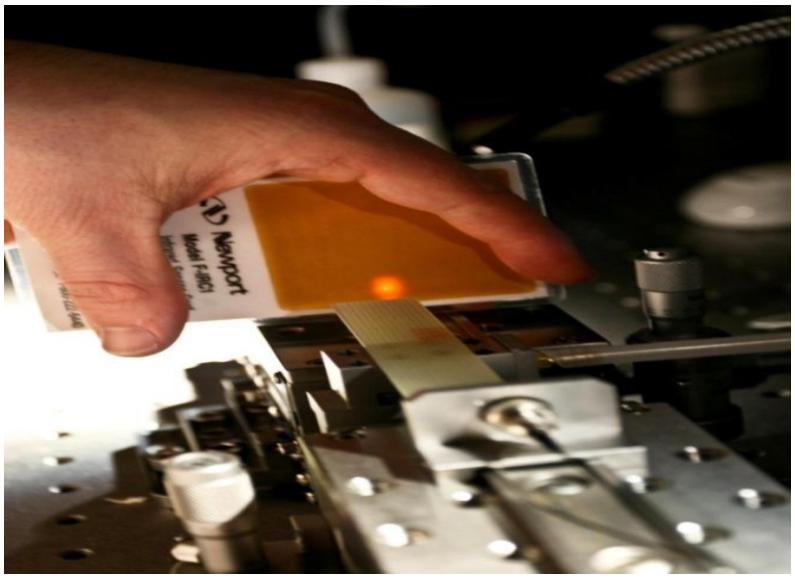

Figure 16: Direct Coupling into Waveguide Core

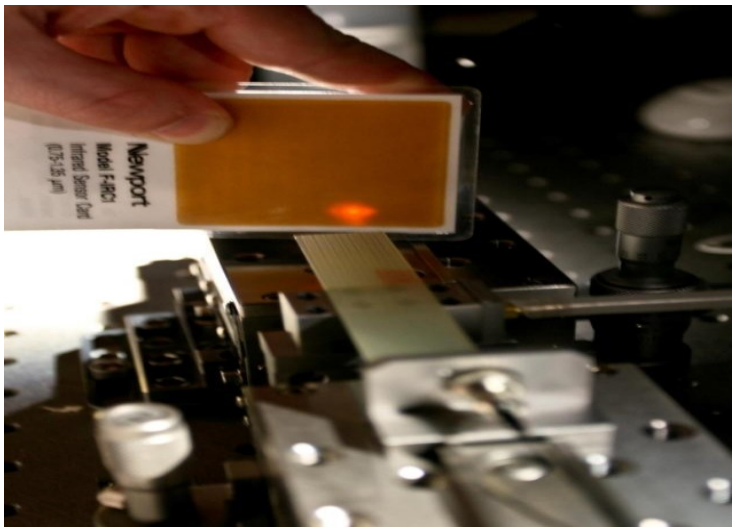

Figure 17: Light Propagation through Waveguide Cladding

Once the input fiber is coupled to the multimode waveguide, a 62.5µm fiber is connected to the output of the waveguide (Figure 18). The input fiber and output fiber are then micro manipulated to achieve the highest output power read from the silicon detector head.

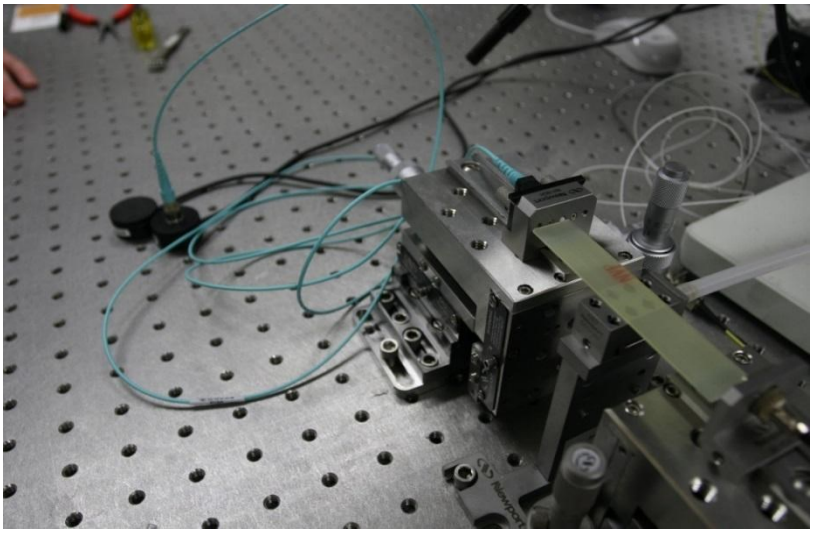
Figure 18: Receiving Fiber and Silicon Power Head

3.2 Optical Waveguide Loss Spectrum

The direct coupling method allows accurate measurement of propagation loss of a single wavelength of light but has to be repeated for each additional wavelength of interest. For optical propagation, the typical wavelengths of interest are 850 nm, 1310 nm, 1550 nm,

as well as 980 nm for emerging VCSEL devices and ~650 nm for plastic optical fiber (POF) applications. Since multiple measurements are time consuming, an effective method to estimate the waveguide losses at each wavelength was developed. Using a UV-VIS-NIR spectrophotometer and a fiber coupled white light source, the direct coupling method can be utilized to measure the spectral losses of the polymer waveguide (Figure 19).

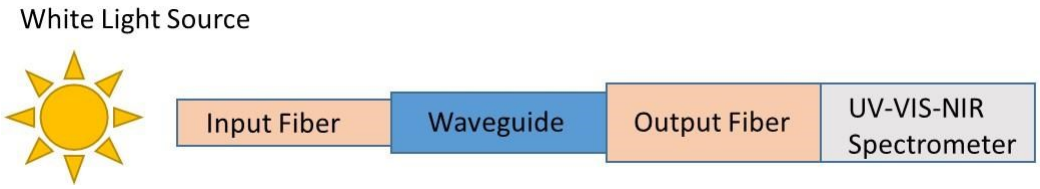

Figure 19: Waveguide Spectrum Loss Schematic

To achieve sufficient white light transmitting through the input fiber, A 50 µm 0.22 NA multimode mode fiber operating was used as the input and a 100 µm 0.27 NA multimode fiber acted as the receiver for the light transferred through the waveguide. With the utilization of the larger input fiber and higher NA, there is coupling loss between the input fiber and polymer waveguide. To compensate for this, the measurement taken at 830 nm using the direct coupling method acts as a baseline shift to match the spectral propagation losses to the narrow linewidth losses. Since the NA of the fiber/ waveguide is different at different wavelengths, coupling losses can be different, Therefore, this method can be used as only an estimation for spectral losses and to measure optical changes in a waveguide. An example of this estimation is in Table 1 where the narrow linewidth and spectral measurements for 830 nm, 1310 nm, and 1550 nm are shown for a polymer waveguide sample where is observed that the 1310 nm and 1550 nm spectral measurements do deviate from their expected values by 5.9 % and 8.8 % respectfully.

Table 1: Measured Values of Narrow Linewidth and Spectral Attenuation

Wavelength (nm)	830	1310	1550
Measured Narrow Linewidth Attenuation (dB/cm)	0.035 ± 0.001	0.345 ± 0.015	1.7 ± 0.15
Estimated Attenuation from Spectrum (dB/cm)	0.035 (baseline shift at this wavelength)	0.036	1.55

% Deviation (%)	0	5.9	8.8

4 Measurement and Analysis

The materials used for this research are a UV photodefinable optical core and cladding material provided by Dow Corning Corporation, specifically Dow Corning ® OE-4140 UV-Cured Optical Elastomer Core and Dow Corning® OE-4141 UV-Cured Optical Elastomer Cladding. These optical silicones have been proven functional and stable in PWG manufactruing by multiple other groups [6]. However, to be successful in industry applications these materials must be well understood to support multiple fabrication processes and environmental impacts that may be present.

4.1 Optimization of Optical Waveguide Fabrication

To produce a 90 µm waveguide stack with 50 µm tall polymer waveguides, the recommended fabrication process of the silicone material on Silicon provided can be found in Table 2. The purpose of the pre bakes of the material is to remove the residual solvent toluene that is carried in the silicone materials for viscosity tailoring. UV exposure is used to initiate the curing of the silicone and the final bake step is to thermally drive the curing to completion for each layer of material. The final oven bake step completely cures the entire waveguide build, creating a stable optically functional material. This section describes analyses performed to optimize the fabrication parameters above for waveguide builds.

Table 2: Standard Spin Recommendations for OE-XXXX Materials on Silicon

Step	RPM	RPM/s	Spin Time	Material		UV Dose	Temperature	BakeTime
Clad pour	0	0	15	Core				
Clad planarize	400	200	60	none				
Bake-HP							110C	2min
Exposure		Flood/Pattern	(F/P)	F	Power (J/cm2)	1.2		
Bake-HP							110C	2min
Core pour	0	0	15	Core				
Core planarize	200	200	60	none				
Bake-HP							110C	2min
Exposure		Flood/Pattern	(F/P)	P	Power (J/cm2)	0.8		
Bake-HP							110C	2min
Mesitylene Pour	0	0	120	Mesitylene				
Mesitylene Pour	250	200	5	Mesitylene				
IPA Pour	250	200	5	IPA				
Wafer Clean	1500	500	30	none				
Bake-HP							110C	2min
Clad pour	0	0	15	Clad				
Clad planarize	400	200	30	none				
Bake-HP							110C	2min
Exposure		Flood/Pattern	(F/P)	F	Power (J/cm2)	1.2		
Clad pour	0	0	15	Clad				
Clad planarize	400	200	30	none				
Bake-HP							110C	2min
Exposure		Flood/Pattern	(F/P)	F	Power (J/cm2)	1.2		
Bake-Oven							130C	30min

4.1.1 Material Prebake

First, the amount of time required to remove all of the excess toluene from the materials in the pre bake step was analyzed. Both core and clad are carried in 30% toluene by

weight, so the core material was used in this analysis, due to the slower spin rates leaving more residual solvent in the material after spinning, making the required core bake times the worst case scenario. Nine wafers were weighed, and then OE-4140 was spun on at 200 RPM. The wafers were weighed, then hot plate baked at surface temperatures of 60C, 90C, and 110C; the weights were measured at incremental times up to 10 minutes. The final wafers were subjected to a 150C bake for 2 hours and measured for a final solvent free weight. Removing the wafer and nonvolatile material weight, the % toluene by mass could be calculated from the measurements. Figure 20 shows that there still is residual toluene in the core after a 2 minute hot plate bake. To optimize the materials to be solvent free prior to curing, a bake of longer time, such as 5 minutes at 90C-110C will be sufficient to remove the excess toluene. This of course is substrate dependent so the surface temperature of the substrate is the value of interest.

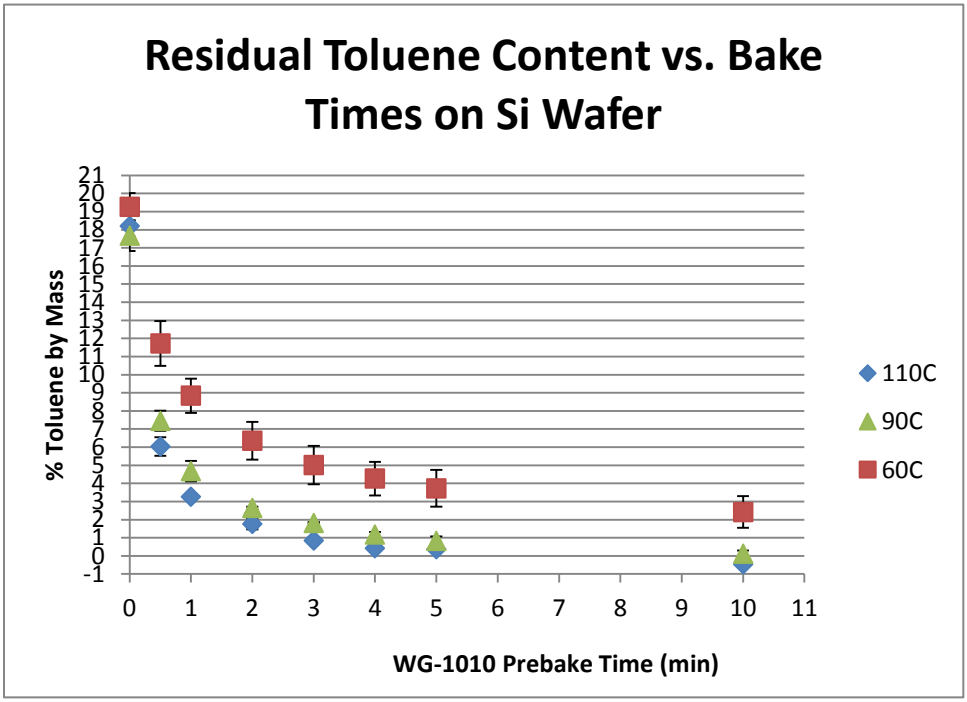

Figure 20: Core Solvent Content During Prebakes

Next, since the waveguides being produced in the recommended process still contain ~1.5%-2% toluene, it was necessary to measure if the toluene had any impact on the optical functionality of the silicones. To address the impact of the toluene, four multimode waveguide builds were performed, varying the core prebake time, correlating to specific % toluene by mass left in the silicone during photopatterning. Core prebakes of 0, 0.5,1, and 2 minutes were performed on separate builds and the cross sections and insertion loss values were taken for analysis. Figure 21 shows the cross sections of the waveguide builds, it can be seen that photo responsively of the material increases with the presence of excess toluene. This is likely due to the lower viscosity of the core layers with more toluene, which can increase the likelihood of crosslinking of the polymer, speeding up the photocuring of the core material.

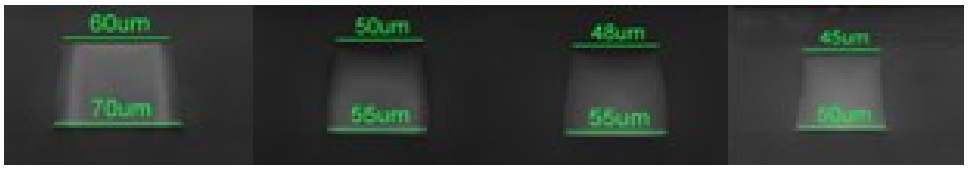

Figure 21: Cross Sections for Various Core Prebake Times (0, 0.5,1,2 min)

Additionally, optical insertion loss measurements were taken for each sample. Sets of 12 waveguides, 10 cm in length were measured at 850 nm using SM direct coupling insertion loss. To compensate for the large size of the 60 µm polymer waveguide, a 100 µm receiving fiber was used. Figure 22shows the average optical loss of the polymer waveguide sets with respect to the prebake time that the core was subjected to, which shows that there is an impact of core prebake on optical functionality.

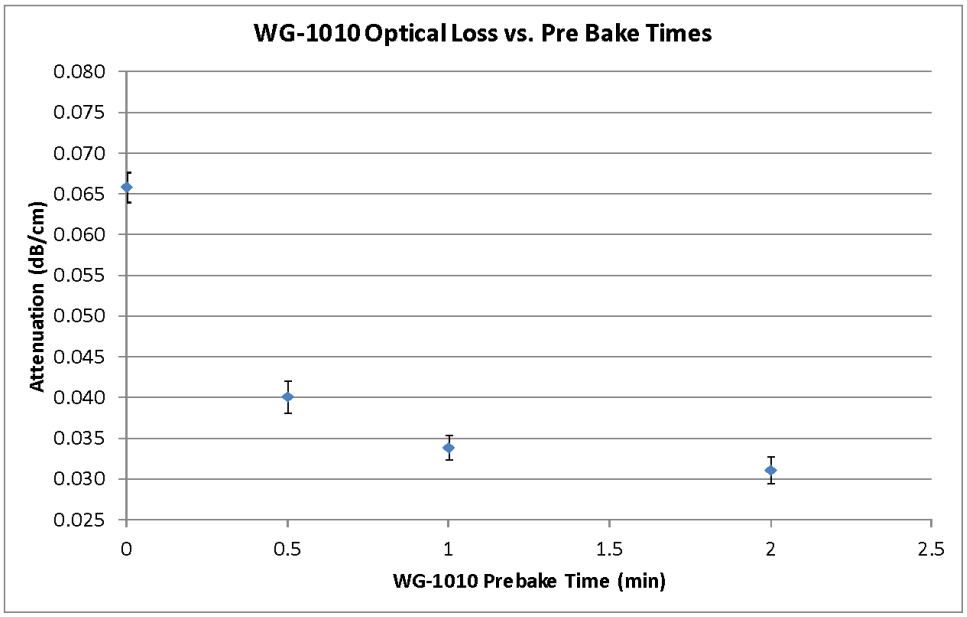

Figure 22: Waveguide Insertion Loss w/ Various Core Prebake Times

Relating Figure 20 and Figure 22, Figure 23 shows the relationship between the excess % toluene by mass and optical loss of the core material. It's clear that there is a direct linear relationship between optical losses and toluene content during the pre exposure bake of the core materials. The graph also shows the possibility of increased optical functionality of the materials, by extending the core prebake time to remove the remaining toluene. It is unclear, however, if this is attributed to excess absorption losses or induced scattering.

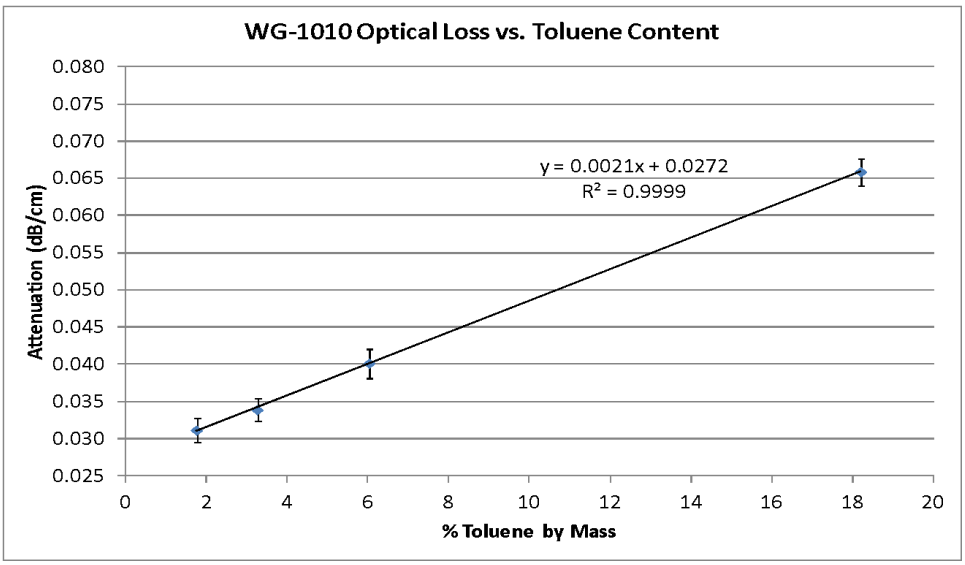

Figure 23: Waveguide Loss w/r to Toluene Content Prior to UV Patterning

Taking an FTIR spectrum of toluene shows no excess absorption at 850 nm due to the molecule driving the assumption of the excess losses to be due to scattering from either the toluene itself or voids it produces in the silicone. The optical crosstalk, which is directly linked to scattering losses, does show an average increase (Figure 24) with respect to toluene content. These values however, are estimations and all fall within one standard deviation of one another, so it cannot be said for certain that optical waveguide scattering is the contributor to the excess losses.

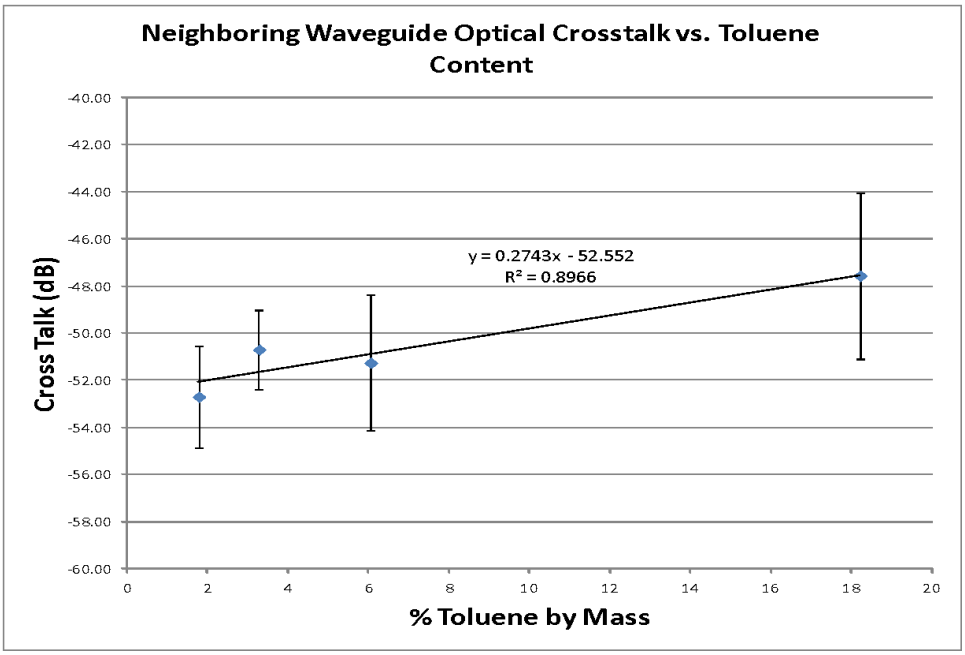

Figure 24: Waveguide Crosstalk w/r to Toluene Content Prior to UV Patterning

The cladding material was also analyzed for performance w/r to toluene content left during prebake. The analysis as to the extent of toluene that is incorporated in the cladding material was not performed, but the functionality w/r to the same bake times the core material was subjected to was performed. Due to the higher RPM for cladding spins and the same amount of % toluene in the both silicone materials, it can be assumed that there is less toluene in the cladding during bakes as demonstrated in the core in Figure 20. Figure 25 shows the surface of cladding layers that have been prebaked at 0, 0.5,1,2 minutes respectively, UV cured, and post baked. It can be seen from the figure that not removing toluene from the cladding material prior to UV curing is detrimental to the mechanical performance of the cladding layers. Although the material cracked slightly at 0.5 minutes, there was no optical performance difference between any of the sample sets minus the sample with no lower cladding prebake, which was destroyed.

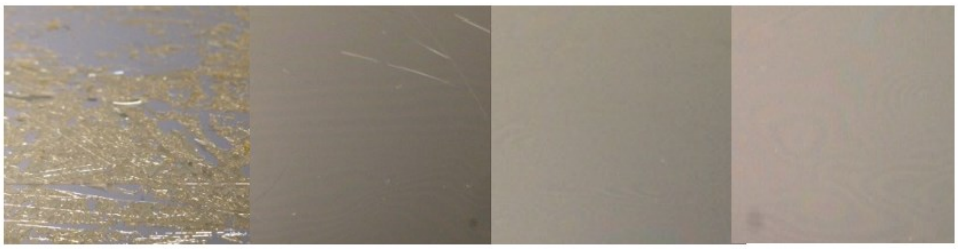

Figure 25: Cladding Surface after Baking at Various Prebake Times (0, 0.5,1,2 min)

4.1.2 UV Dose

Understanding the relationship between UV dose and the resulting lithographic pattern of the core material was the next step for optimization of fabrication of the polymer waveguides. Figure 26 the sensitivity of the core material and the UV bulb being utilized for this analysis, which shows that 365 nm peak of the bulb and material sensitivity overlap. To further understand the impact of the UV dose, 3 core silicone materials with varying ratios (1, 1.5, 2:1) of photoinitiator to the standard material were utilized.

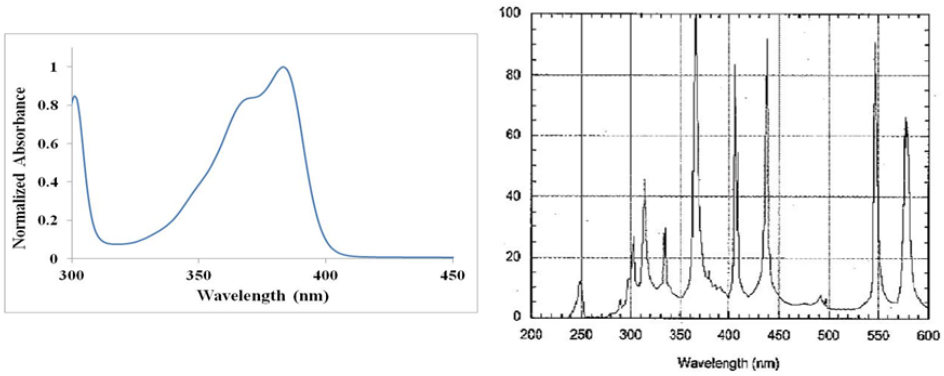

Figure 26: Normalized Sensitivity of Core/Clad Photoinitiator (Left), Normalized Output Spectrum of Photolithographic Bulb (Right)

To understand the relationship of UV dose to patterning of a material, a variable exposure mask was used, which was comprised of 10 sections on a lithographic mask with optical transmission percentages of 30%-100% (Figure 27). In each transmission window there are 50 µm square features, which allows the user to fabricate features in a material that has be dosed 30%-100% of the expected dose on a single lithographic process.

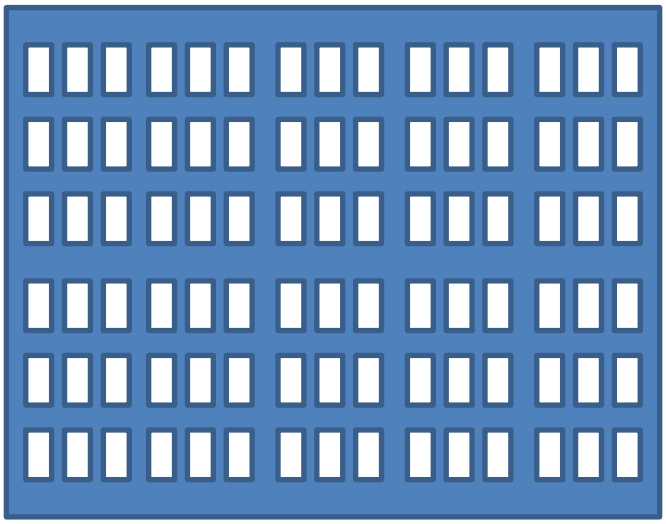

Figure 27: Schematic of Variable Exposure Mask with Transmission from 30%-100%

Taking a standard core material spun on Silicon, these 50 µm square features were fabricated on Silicon wafers and measured via top down optical microscopy. Figure 28 shows an example of the polymeric squares measured in the analysis. Performing the builds and taking the square sizes, Figure 29 shows the dependency of feature size w/r to dose and photoinitiator concentration. It can be seen that over a large range of UV dose, the only material that reaches the desired 1:1 patterning ratio is the standard 1x photoinitiator concentration. The recommended dose for the correct feature size however,

is almost double what is currently being used; also demonstrating that 0.8 J/cm^2 dose produces 45 µm features with the current UV configuration.

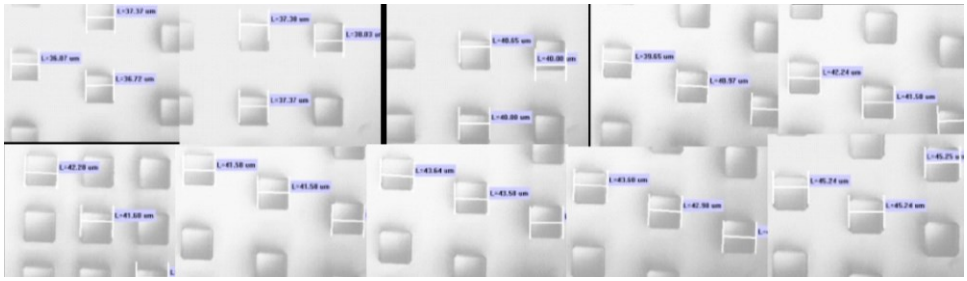

Figure 28: 50 µm Square Features from 30%-100% of a 2.4J/cm2 Dose in Core Material

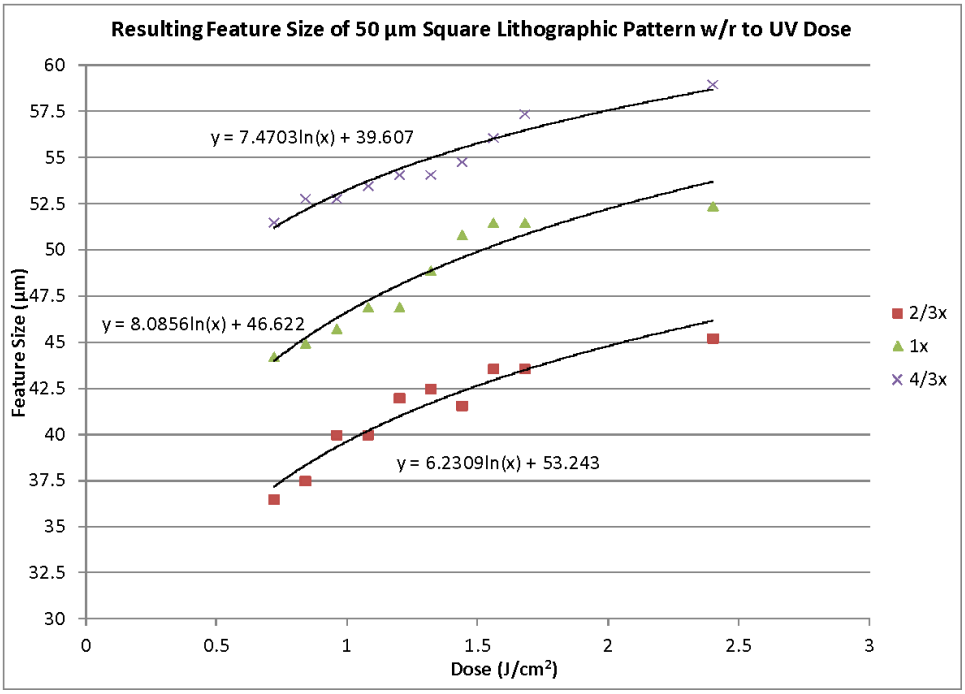

Figure 29: Resulting Feature Sizes vs. Dose for 3 Variations in Photoinitiator Concentrations in Core Material

4.1.3 Core and Clad Post Bake

Post bake analyses were performed on the lower cladding and core materials to assess the impact they have on opto-mechanical functionality of the polymer system. It was assumed that since the final bake step came directly after the post exposure bake of the upper cladding material, that this step was unnecessary. However, the post exposure bake on the lower two layers, impacts adhesion and waveguide formation. First, the lower cladding was analyzed. Similar to the prebake analysis, four waveguide builds were fabricated changing the post exposure bake step to 0, 0.5,1,2 minutes.

These builds were cross section imaged and insertion loss was tested. Figure 30 shows the cross sections for the waveguide builds (2 minutes cross sections not available), and it can be seen that there is a stretching of the polymer waveguide bottoms when the lower cladding isn't fully polymerized. When the post exposure bake is increased on the lower cladding the stretching of the core is lessened. This suggests that to obtain the symmetric features required for optimal signal transmission, the lower cladding should be post exposure baked to final cure completion. Continuation of the post exposure bake of the lower cladding (5+ minutes) prior to core deposition did show degradation in adhesion between core and cladding so there are inherent limitations to the amount of cure the lower cladding should be subject to. Optical insertion loss analysis of the four builds showed an improvement (Figure 31) with less post exposure baking of the lower cladding, although measurements are suggestive at these small differences in attenuation with the current testing methods.

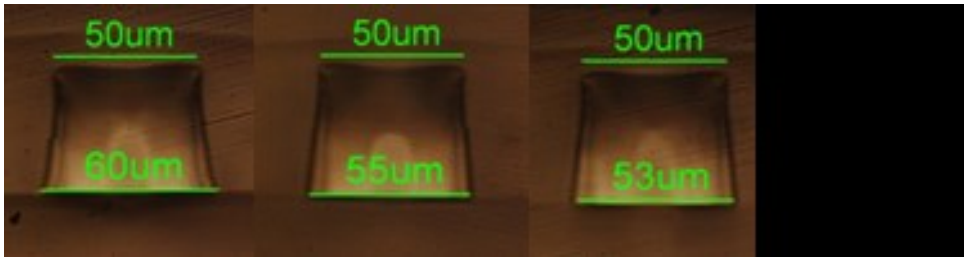

Figure 30: Core Cross Section Images Varying Lower Cladding Post Exposure Bake (0, 0.5,1,2 minutes)

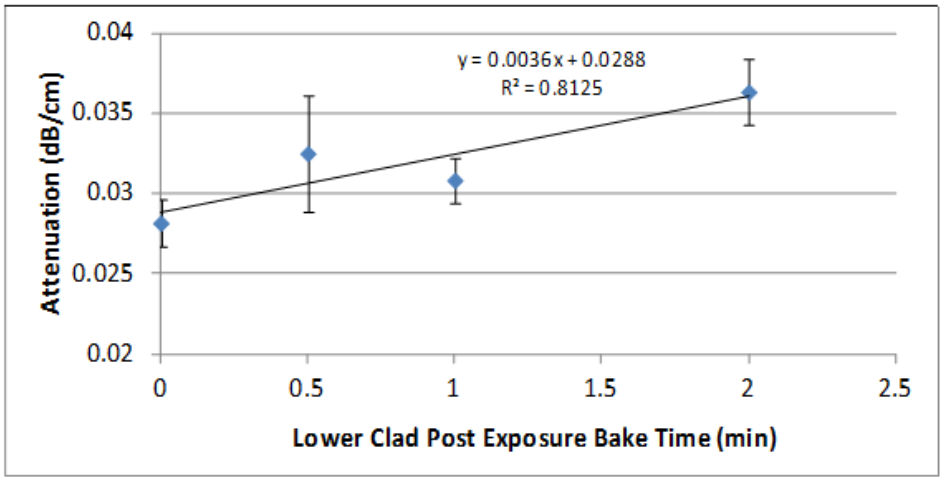

Figure 31: Optical Insertion Loss Varying Lower Cladding Post Exposure Bake Times (0, 0.5,1,2 minutes)

Performing the same analysis on the core post exposure bake netted similar results, Figure 32 shows the cross section images with varying core post exposure bake times with the 0 second post exposure bake completely developing away the patterned waveguides. It is observed that when the core is at a lower curing state, much more swelling and stretching is apparent in the material, but stabilized after 1 minute post

exposure bake. Similarly, Figure 33 shows optical insertion losses amongst the group equalize after 1 minute post exposure bake of the material suggesting that 1 minute is sufficient for optical functionality.

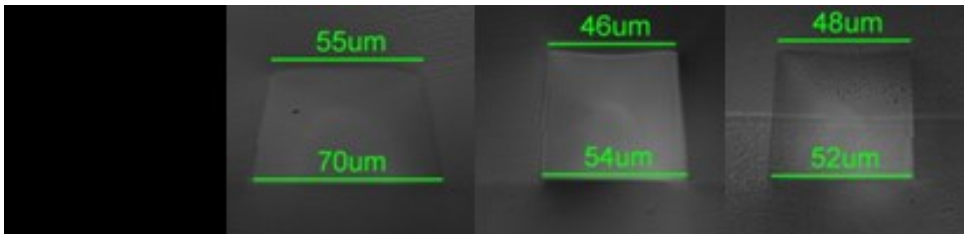

Figure 32: Core Cross Section Images Varying Core Post Exposure Bake (0, 0.5,1,2 minutes)

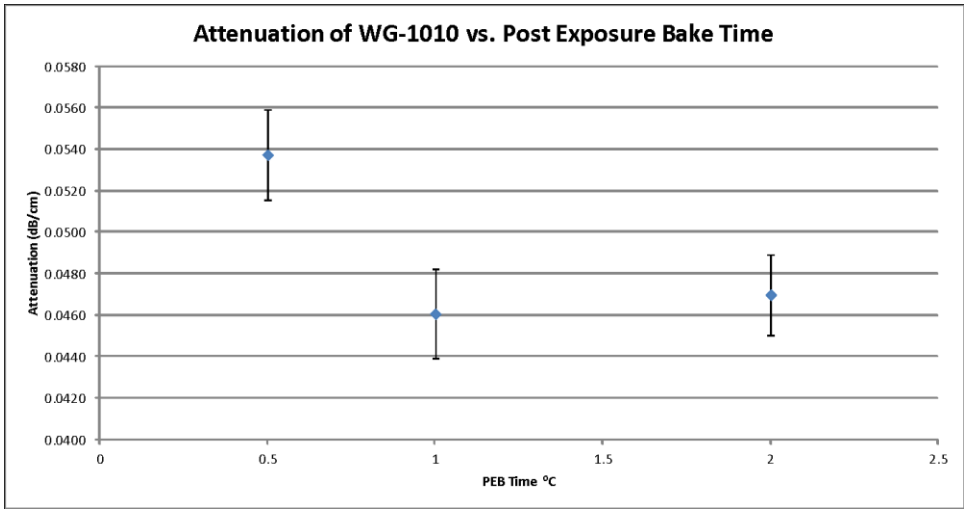

Figure 33: Optical Insertion Loss Varying Core Post Exposure Bake Times (0, 0.5,1,2 minutes)

4.1.4 Solvent Development

Although not addressed in this thesis, concerns of large quantities of aggressive solvents in industry (PCB, Semiconductor, etc.) are apparent. An assessment was performed to address the viability of using alternative development solvents with lower hazard ratings if certain solvents weren't accepted in industry. Table 3 shows solvents that have been shown successfully to act as a development solvent for the patterned core materials along with their associated hazards, showing that safer alternative solvents can be utilized as developing agents for these material sets.

Table 3: Alternative Solvents List for Core Pattern Development

Solvent	Flash Point (°C)	Hazard

Mesitylene	53	GHS02,07,09
MIBK	14	GHS02,07
Acetone	-17	GHS02,07
Butyl Acetate	23	GHS02,07
Butoxyethoxl Ethyl Acetate	102	
Diethylene Glycol Monoethyl Ether Acetate	98	GHS07
PGMEA	43	GHS02

4.1.5 Final Hard Bake

Final hard bake requirements were analyzed to assess the impact that a final bake has on the functionality of the material set. A full polymer waveguide build was fabricated on Silicon and diced prior to the final hard bake. One portion of the diced sample was subjected to the 30 min 130°C bake and the other was not. Both samples were tested for optical insertion losses and subjected to thermal aging to address if they were indeed optically stable. 2000 hours of 85°C/85%relative humidity (RH) was applied to the optical waveguides, being optically tested at 250, 500, 1000, and 2000 hours. Figure 34 shows the results; out to 2000 hours both material sets remain optically functional making the final hard bake from an optical standpoint not necessary.

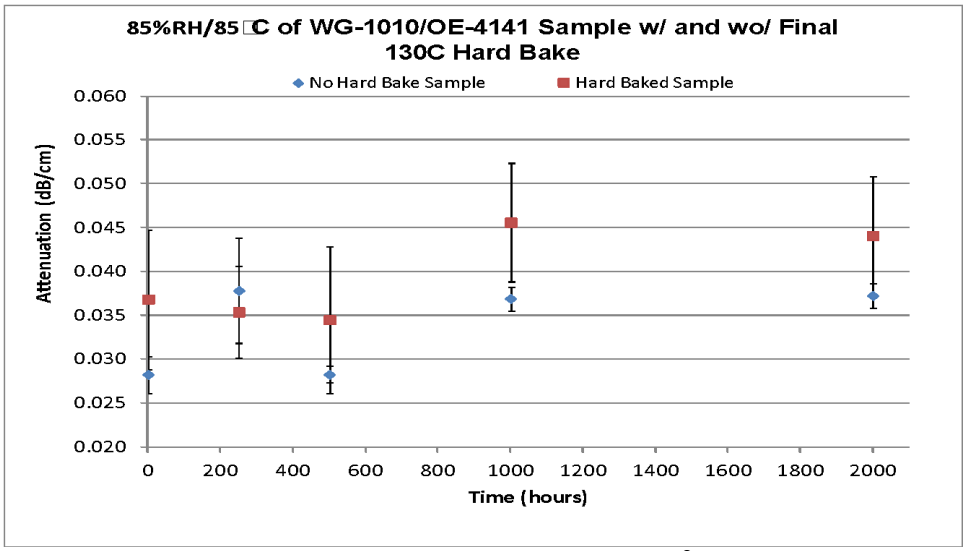

Figure 34: Optical Loss Testing of Samples Subjected to 85°C/85%RH w/ and w/o Final Hard Bake

Further testing of the optical properties due to the final hard bake, optical waveguide loss spectra were taken to address the effects on optical performance in the NIR. Figure 35 shows that the majority of NIR wavelengths are unchanged over the lifetime of these materials, slight increases are present in the 900 nm-1100 nm bands that would have to be addressed if the wavelengths of interest fell within this scope. Typically 850, 1310, and 1550 nm are transmission wavelengths of interest which are unaffected, but VCSEL wavelengths of 980 nm are active in industry as well.

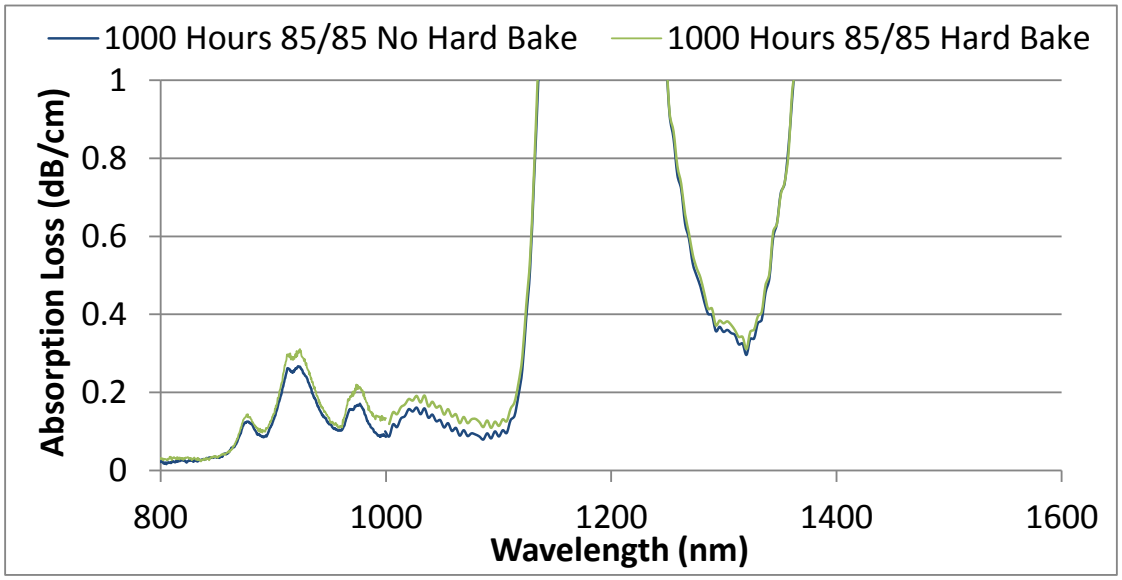

Figure 35: Optical Waveguide Loss Spectrum of Samples Subjected to 1000 hours 85C/85%RH

4.1.6 Optimized Fabrication Parameters

Based on the results of the analysis, optimized fabrication parameters were developed. Table 4 shows the changed parameters to optimize polymer waveguide functionality. Full waveguide builds were fabricated with the specified parameters to verify optical functionality and structure.

Table 4: Optimized Fabrication Parameters of OE-XXXX Materials on Silicon

Step	RPM	RPM/s	Spin Time	Material		UV Dose	Temperature	BakeTime
Clad planarize	400	200	60	Clad				
Bake-HP							110C	3min
Exposure		Flood/Pattern	(F/P)	F	Power (J/cm2)	1.2		
Bake-HP							110C	3min
Core planarize	200	200	60	Core				
Bake-HP							110C	5min
Exposure		Flood/Pattern	(F/P)	P	Power (J/cm2)	1.5		
Bake-HP							110C	1min
Butoxyethoxl Ethyl Acetate Pour	0	0	120	Butoxyethoxl Ethyl Acetate				
Butoxyethoxl Ethyl Acetate Pour	250	200	5	Butoxyethoxl Ethyl Acetate				
IPA Pour	250	200	5	IPA				
Drying Spin	1500	500	30	none				
Clad planarize	400	200	60	Clad				
Bake-HP							110C	3min
Exposure		Flood/Pattern	(F/P)	F	Power (J/cm2)	1.2		
Clad planarize	400	200	60	Clad				
Bake-HP							110C	3min
Exposure		Flood/Pattern	(F/P)	F	Power (J/cm2)	1.2		

4.2 Substrate Selection

In the printed circuit board industry, the most common type of substrate for electrical insulation is glass resin epoxy. This is often denoted by its grade, which the majority of industry uses FR4 grade glass resin epoxy. Other laminates, such as polyimides, ceramics, glasses, and others are often utilized as well for specialty markets where their unique characteristics are required. These specialty laminates will not be studied and this research will stay within the area of generic FR4 laminates.

There are many grades and types of FR4 as well, tailoring to different industry requirements such as halogen free, high speed, low/high thermal conductivity, RF specific, low signal specific, etc. which vary amount and compositions of materials to tailor these. It would be an unreasonable assumption that all of these can be addressed in this thesis, so the focus will be on the two largest available FR4 materials, halogen and halogen free FR4 laminates. The difference between the two materials is that generally the flame retardants used to make FR4 are brominated chemicals, and have been shown to be hazardous. Non-hazardous halogen free FR4 materials use alternative flame retardant agents limiting the amount of brominated/chlorinated content to 1000ppm in printed circuit boards. One of the concerns for optical stability of polymer waveguides in printed circuit boards is the affect these flame retardants have on the material performance demonstrated in Figure 36 that could potentially impact optical functionality of the optical layer.

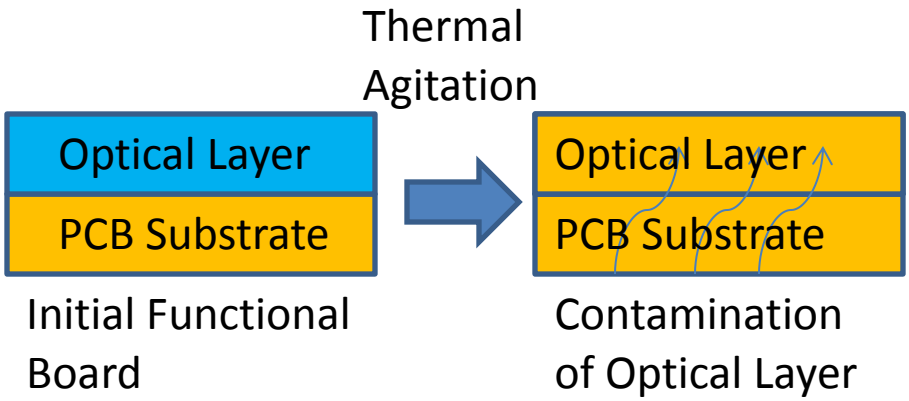

Figure 36: Possible PCB Contamination of Optical Layer

To address this, first the weight loss of a standard FR4, halogen free FR4, and a Silicon wafer were taken to address the amount of material lost in each substrate. Thermal ramp rates of 10C/min were applied to the 3 substrates in Nitrogen, and their weight losses analyzed. The ranges of temperatures for the weight loss analysis were picked for the maximum bake temperature of the polymer waveguides (130°C), typical wave soldering maximum temperature (260°C), and common manual reflow soldering temperature (350°C). It can be seen in Table 5 that the materials are stable for the optical waveguide builds to 130C, but start exhibiting weight loss up to wave reflow, and significant degradation at manual solder reflow temperatures.

Table 5: Weight Loss Analysis of Common PCB Substrates

Sample	**1st Wt. Loss (25C-130C) (Wt. %)**	**2nd Wt. Loss (130C-260C) (Wt. %)**	**3rd Wt. Loss (260C-350C) (Wt. %)**	**Final Residue (Wt. %)**	**Onset of Degradation (°C)**
FR-4 Halogenated	0.00	0.10	13.4	87.2	345
FR-4 Non-Halogenated	0.00	0.28	11.1	89.3	291
Silicon Wafer	0.00	0.00	0.00	100	-

Since the materials do exhibit weight loss at wave soldering temperatures and would likely be subjected to wave reflow environments, waveguide builds were fabricated on the three substrates and measured for optical losses. The samples were then subjected to a typical wave solder reflow profile seen in Figure 37. This profile consists of a 130°C ramp, 225°C soak, 260°C reflow, and two cooling steps. The reflow was applied to the samples 5 times, corresponding to a likely maximum amount of solder cycles that the materials would ever be subjected to in practice.

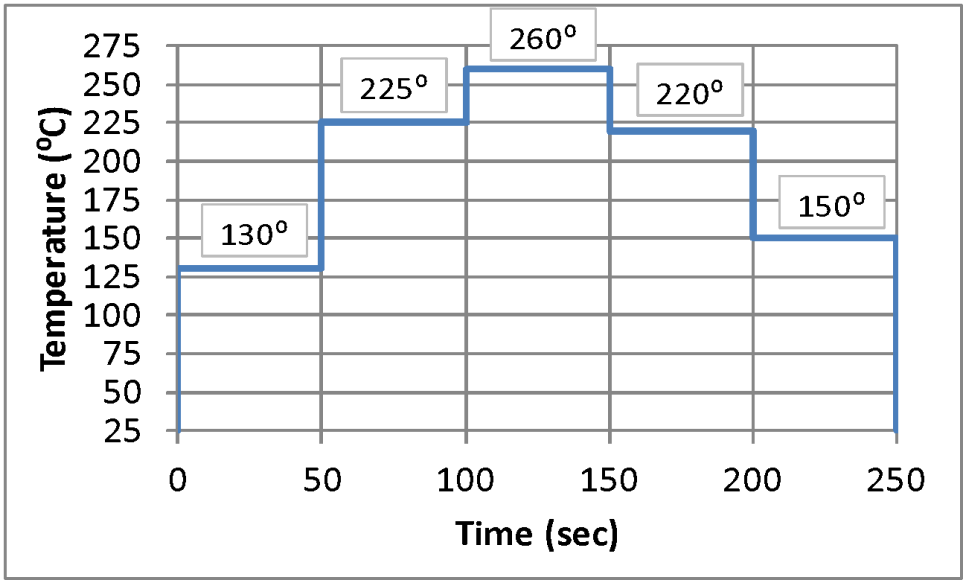

Figure 37: Solder Reflow Profile for Analysis

With the silicon substrate serving as a baseline for material based losses due to the solder profile, Figure 38 shows optical attenuation changes for the three materials. Silicon and halogenated FR4 are indistinguishable while there is a clear increase in optical losses due to the halogen free substrate. It is unclear if the components used for the flame retardation affect optical performance more than the brominated components, or if it is solely due to the amount of diffusion present at the reflow temperature. Optical cross talk of all three measurements was unchanged as well; suggesting the increase in loss was due to material absorption.

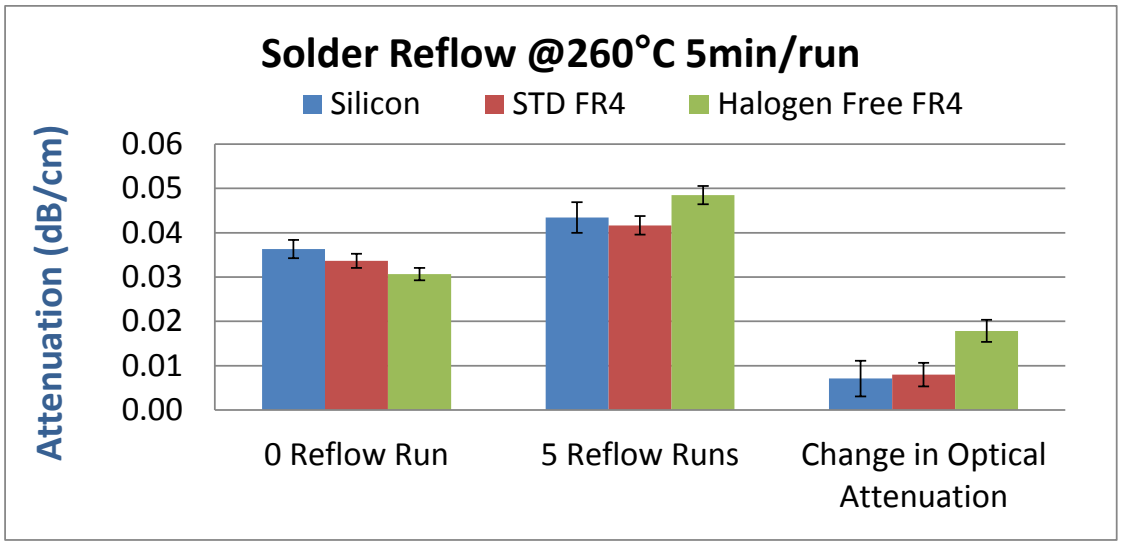

Figure 38: Change in Attenuation after Solder Reflow on Various Substrates

It is also assumed that since the flame retardants are meant to thermally diffuse in events of higher temperatures that they are free floating in the glass resin epoxy or their molecular bonds break at low energies. Random diffusion of the retardants over time could lead to degradation of optical functionality over long operational lifetimes, driving a need for correct substrate selection. 85/85 testing was performed on the manufactured waveguide builds to assess the impact that the PCB substrates would have on optical performance. Figure 39 shows the results of optical performance out to 2000 hours subjected to 85/85 testing. It is shown that there is a clear increase in halogen free FR4 substrates over the lifetime of the material operation. It also appears that the FR4 substrate was following the same trend of the halogen free but after 500 hours was depleted and returned to the baseline. This suggests that there is a common diffusing element in both materials that depletes in the standard FR4 over time. Further analysis of this effect and mitigation of the chemical element could remove this increase in optical losses of halogen free FR4 substrates.

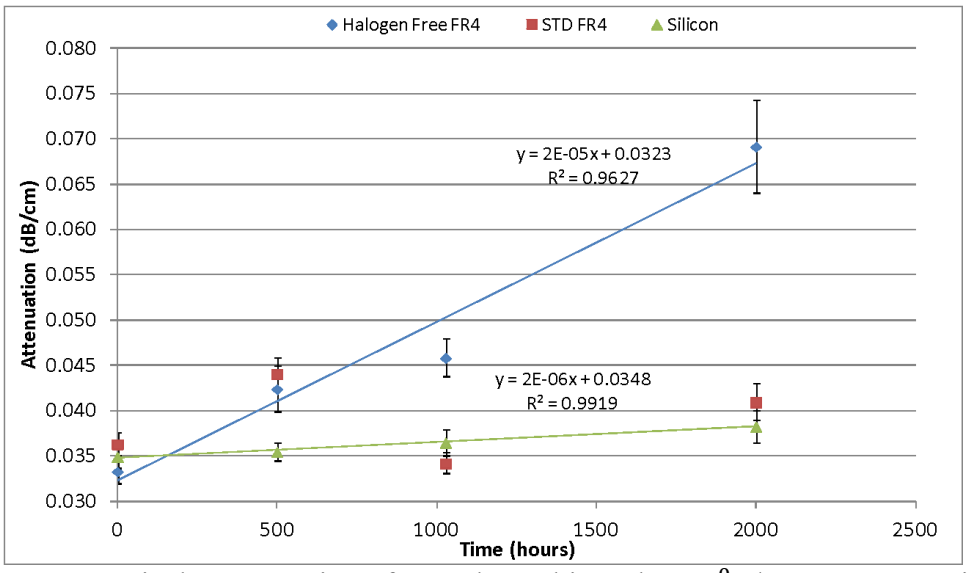

Figure 39: Optical Loss Testing of Samples Subjected to 85°C/85%RH on Various Substrates

Manufacturing, transfer, and housing of glass reinforced epoxies have multiple requirements due to possibilities of moisture contamination, which can adversely affect integration of electronics onto the board. Standards currently exist regarding the handling of FR4 laminates to address contamination issues, one of which is a dehydration bake on the FR4 laminate to remove liquid contamination. Standard practices vary based on substrate thickness, material, and technology but baking of substrates prior to integration at 125°C from 3-48 hours is common.

To test the effects that the dehydration bake has on optical functionality of the materials, a 130C dehydration bake was applied for 48 hours to boards, then were fabricated again and optical testing was repeated. Solder reflow and 85/85 testing was performed on the dehydrated waveguide builds. Figure 40 shows the results from 5 solder reflows, demonstrating an improved performance in the halogen free FR4 samples and no change in the baseline and FR4 sample.

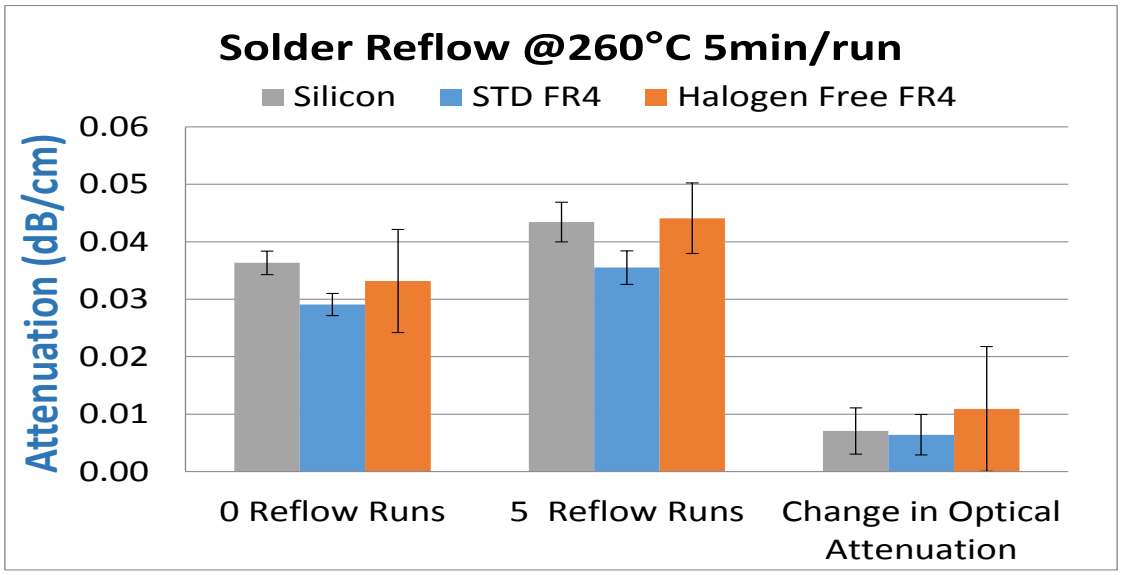

Figure 40: Change in Attenuation after Solder Reflow on Various Substrates w/ Dehydration Bake

85/85 analysis showed similar improvements in both the FR4 and halogen free FR4 samples. It can be seen in Figure 41 that the optical signal quality for all three substrates is within 1 standard deviation of one another. Also, relating Figure 39 and Figure 41, there is no significant increase in optical losses over time on the halogen free FR4 materials as there was without a substrate dehydration bake.

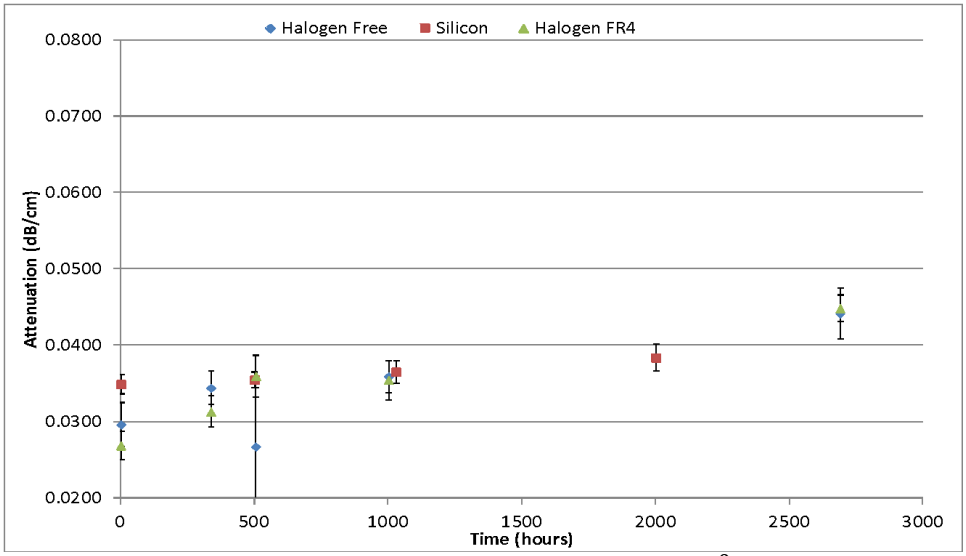

Figure 41: Optical Loss Testing of Samples Subjected to 85^0C/85%RH on Various Substrates w/ Dehydration Bake

Substrate selection has been shown to be an integral part for OEPCB integration. Future developments call out for optical layers to be integrated into PCB layers which are comprised typically of glass reinforced epoxies. Flame retardants, contaminates, and

moisture all have an impact on functional performance of electrical, as well as optical components. Mitigation techniques and further baseline analysis of substrates will need to be performed to understand and eliminate the root cause for optical functionality degradation.

4.3 Board Integration [28]

If the implementation of polymer optical waveguides in printed circuit boards does not require embedding the optical layer into the EOPCB (Figure 42), waveguide layers only have to withstand operational lifetimes and reflow processes discussed above. Realistically, surface board space is extremely populated, so for low density optical interconnections, top surface optical layers may be possible but for most applications where the benefit of polymer waveguides is high density, this is not applicable. Optical flyover ribbons however, could be the first step in commercialization, leading to full board integration, therefore the materials could be utilized for such a technology.

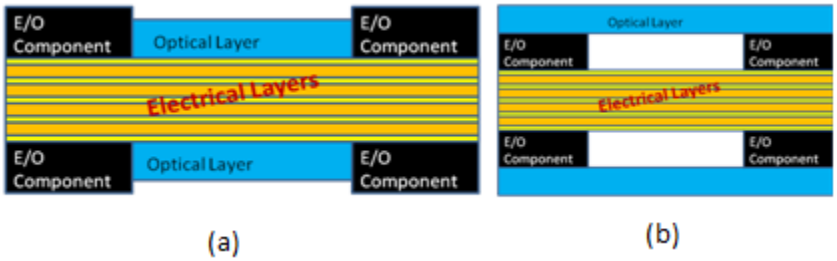

Figure 42: Theoretical Cross Section of on Surface Optical Layers (a) and Flyover Ribbon (b) for Signal Routing

For full embedment of optical layers in PCBs (Figure 43), polymer optical materials will be subjected to chemical, thermal, and mechanical processes that the PCB withstands in fabrication. Although all of the inner layers in a PCB are made separately, the stack of materials are laminated together and run through an assortment of drilling, cleaning, and plating processes to create electrical connections between layers. Understanding the impact that these processes have on the polymers optical performance is crucial for integration of optical layers into EOPCBs.

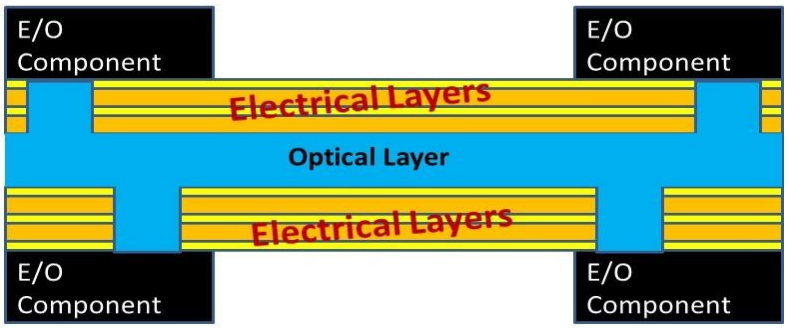

Figure 43: Theoretical Cross Section of Embedded Optical Layer in PCB for Signal Routing

4.3.1 Chemical Analysis & Lamination

Processes associated with multi-layer printed circuit boards are very complex with a multitude of chemical and mechanical steps that vary according to the application, company, and quality. As a high level overview Figure 44 shows step-by-step processing of multi-layer electrical boards. This consists of first the inner electrical layers are independently manufactured. They are then stacked and laminated together with an adhesive, usually an uncured resin consisting of the same components as FR4 that cures during the lamination step. After, drilling and through layer electrical connections are made though an array of chemical steps. For first generation boards, it would be safe to assume that the electrical and optical layers will be fabricated independently (Figure 45) and brought together in the lamination process. Future generations might copper plate the optical layer and utilize it as one of the active electrical layers as well but that is speculation.

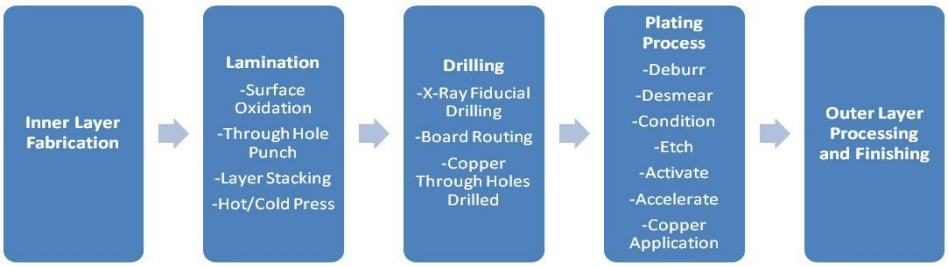

Figure 44: Multilayer Printed Circuit Board Processing

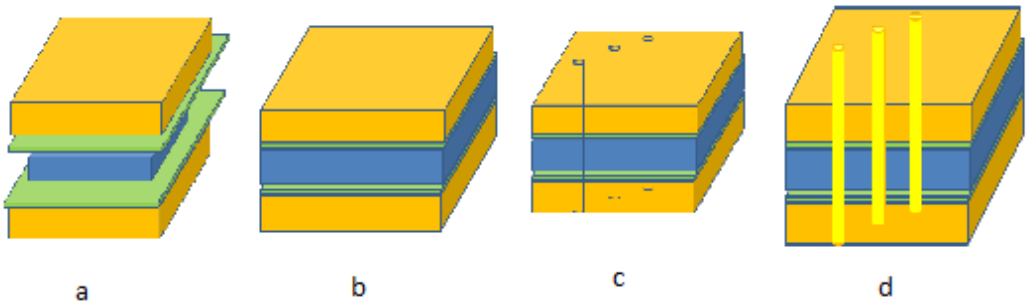

Figure 45:(a) Stacking of Electrical, Optical, and Adhesive Layers; (b) Lamination Process; (c) Drilling; (d) Copper Plating

To test the inertness of the polymer material to the processes associated with lamination and the chemicals used in drilling and plating, sets of polymer waveguide samples were fabricated on FR4 and measured for optical losses at 850nm. They were then subjected to chemical testing. Figure 46 shows two examples of waveguide samples after printed circuit board chemicals were applied.

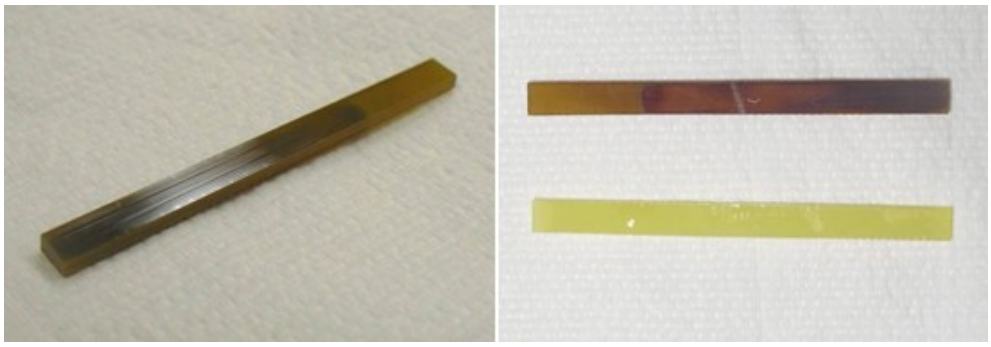

Figure 46: Samples Subjected to a Desmearing Process (Left and Top Right) and an Activation Process (Bottom Right)

The samples were subjected to a standard plating process demonstrated at a private printed circuit board company, so some of the chemical treatment materials are proprietary and cannot be disclosed. But for the scope of this thesis, the specific chemical treatment is not as important as the concept that the process can or cannot be demonstrated, so chemicals will be left in generic terms where necessary. The first set of chemical treatments that were performed were the through hole preparation steps after drilling. This consisted of a smear treatment, removal, glass etch, and board conditioning step.

Table 6: Through-hole Preparation Steps

Step	Chemical	Temp (^{o}F)	Time (min)
Smear Treatment	Glycol Ether(M-Treat AQ), Sodium Hydroxide(M-79224), water	155-180	9
Smear Removal	Potassium Permanganate (M-Permanganate P), Sodium Hydroxide(M-79224), water	160-180	20
Glass Etching	Sodium Bifluoride (M-Glass Etch), Sulfuric Acid, water	85-110	1
Board Conditioning	Potassium Hydroxide, water	125	6

The results shown in Figure 47 show that there is minimal change in optical performance due to all treatments except the smear removal step. These additional losses are expected to be due to the absorption of the Potassium Permanganate that was used in the smear removal process. Figure 46shows the reddening of the desmeared sample that can lead to losses in the NIR spectrum as well as additional scattering losses due to the high refractive index of the material (1.59). The increased losses due to the material however, may not be an issue in a real manufacturing setting as the polymer waveguides will only be subjected to the chemical in areas where through holes are present. More analysis to further explore this chemical's impact will have to be explored.

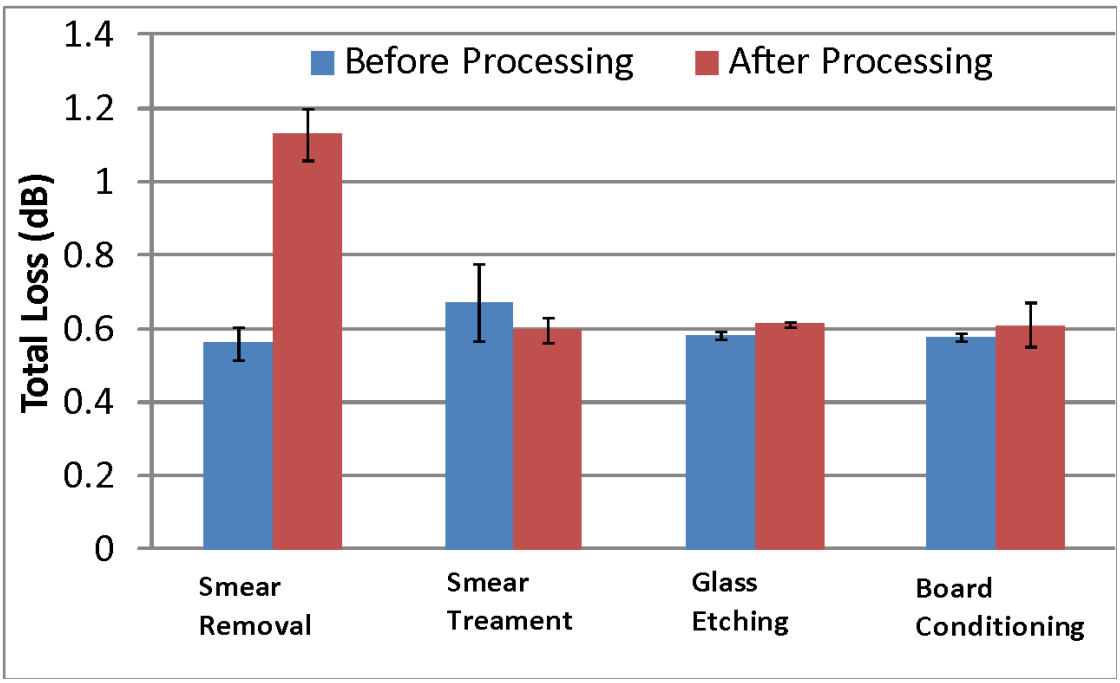

Figure 47: Optical Loss Changes due to Through-hole Preparation

Each sample was also subjected to the copper plating steps outlined in Table 7. These processes consisted of a micro etch, board activation, board acceleration, copper plating, and anti-tarnishing step. The resulting optical loss changes in Figure 48 shows that the materials are inert to these copper plating processing steps.

Table 7: Copper Plating Steps

Step	Chemical	Temp (°F)	Time (min)
Micro-Etching	Phosphoric Acid, Hydrogen Peroxide, Sulfuric Acid, water	125	0.6
Board Activation	Trade Secret Organic Acid, Hydrochloric Acid-Stannous Chloride, Hydrochloric Acid	90	4.5
Board Acceleration	Non-hazardous (M-Accelerate A), Sodium Chlorite	120	2.25
Electroless Copper Plating	Copper Chloride-Formaldehyde. Sodium Hydroxide-Chelator, Sodium Hydroxide, Methanol, Formaldehyde	115	20

Anti-tarnishing	Isoproanol-Potassium Hydroxide, Acetic Acid	85	2.75

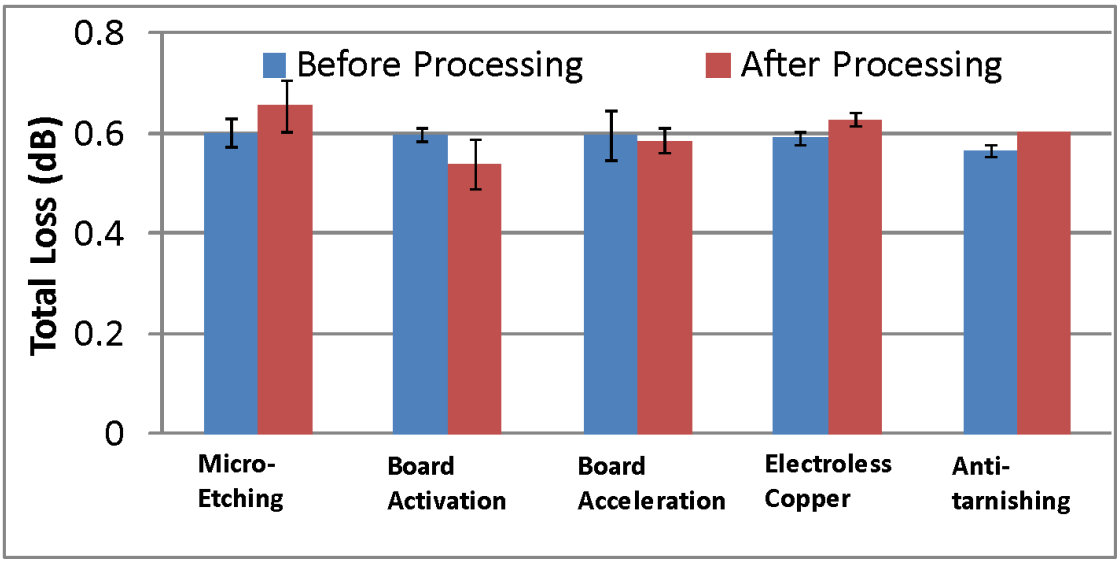

Figure 48: Optical Loss Changes due to Copper Plating Process

To test the effects that high temperature and pressure have on the optical materials, samples on standard and halogen free FR4 were subjected to lamination temperatures of 180C @ 900 N/cm2 for 2 hours. Due to the limitations of the hydraulic press available, 900 N/cm2 was used as the lamination pressure, which is much higher than the 150-350 N/cm2 pressures that would typically be used in industry. Also, Silicon baseline standards could not be used in this measurement due to Silicon's brittle nature. Figure 49 shows the resulting change in optical losses due to the lamination process, indicating an increase in loss for both material sets. To further this work, the lamination process will have to be repeated with a more industry related method of lamination.

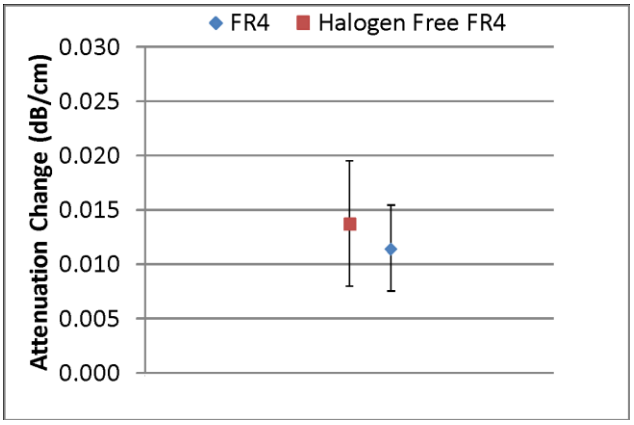

Figure 49: Attenuation Change Due to Lamination Process on Various Substrates

5 Conclusions

The first goal of this research was to understand and optimize the manufacturing process of a photopatternable material that was suitable for polymer waveguide fabrication. The process parameters given for the Dow Corning OE-4141 and OE-4140 material set was shown to not be optimal for optical functionality of the material set. Analyses showed that the given thermal cycle for core to remove toluene left 2% toluene in the layer, and this left over solvent caused a 10% increase in optical loss. Increasing the bake time to further remove solvent in the core layer can improve optical functionality of the material set by up to 10%. The cladding material was also shown to have mechanical degradation if the solvent removal bake wasn't optimized but the post exposure bake had a lesser impact. The final hard bake of the polymer waveguide stack was shown to be unnecessary to stabilize the polymer materials, which allowed a 30-minute reduction in processing time of the materials. Multiple safer solvents were demonstrated to act as developing agents in the manufacturing process as well which can aid in the adoption of the mass manufacturing of this polymer waveguide material.

The second goal of this research was to demonstrate that the material set was robust to standard Telecordia and printed circuit board processes. 85°C/85%RH testing was performed as well as solder reflow on multiple PCB substrates as well as a baseline silicon sample, showing that substrate selection has an impact on the lifetime performance of the material. It was demonstrated that these materials are not stable with standard printed circuit board substrates. A mitigation technique was developed and demonstrated to reduce optical degradation by 0.03 dB/cm due to 85°C/85%RH and 0.01 dB/cm due to solder reflow.

The third goal of this research was to assess the impact that embedment of polymer waveguides into a printed circuit board had on optical functionality. Multiple processes in PCB via preparation and plating were demonstrated to have little effect on the materials performance. The smear removal step in the manufacturing process did have an impact on optical performance but its impact on a real system will have to be further explored. The thermal and pressure agitations of lamination did also show to have an impact on pwg performance, and optimization of these parameters to mitigate that will be explored in future work.

Now that the process for pwg manufacturing has been fully developed and each process step for integration studied independently, future work will revolve around assessing the impact that a real PCB manufacturing process has on pwg performance. Assessment of the optical and mechanical stability and compatibility of the pwg materials will be done on polymer waveguides that go through the entire lamination, via drilling/plating, and solder reflow process. Additional optical measurement parameters such as coupling loss, crossing loss, and numerical aperture measurements will be performed to fully analyze the optical material's performance.

6 Reference List

[1] A.F. Benner, et al. ,"Exploitation of optical interconnects in future server architectures," IBM Journal of Research and Development, vol.49, no.4.5, pp.755, 775, July 2005

[2] K. Hasharoni, et al.,"A 1.3 tb/s parallel optics VCSEL link ", Proc. SPIE 8991, Optical Interconnects XIV, 89910C (March 8, 2014)

[3] D. G. Kam *et al*., "Is 25 Gb/s On-Board Signaling Viable?," in *IEEE Transactions on Advanced Packaging*, vol. 32, no. 2, pp. 328-344, May 2009.

[4] Y. Ban, T. D. Keulenaer, G. Torfs, J. H. Sinsky, B. Kozicki and J. Bauwelinck, "Experimental evaluation of NRZ and duobinary up to 48 Gbit/s for electrical backplanes," in *Electronics Letters*, vol. 51, no. 8, pp. 617-619, 4 16 2015.

[5] https://3s81si1s5ygj3mzby34dq6qf-wpengine.netdna-ssl.com/wp-content/uploads/2016/10/top500-nov-2016-performance-over-time.jpg

[6] Frank Chang; Recent advances of emerging PAM4 signaling with real-time processing for 100/400Gbps data center connectivity. Proc. SPIE 9775, Next-Generation Optical Networks for Data Centers and Short-Reach Links III, 977507 (March 7, 2016);

[7] P. Groumas, Z. Zhang, V. Katopodis, A. Konczykowska, J. Y. Dupuy, A. Beretta, A. Dede, J. H. Choi, P. Harati, F. Jorge, V. Nodjiadjim, M. Riet, R. Dinu, G. Cangini, E. Miller, A. Vannucci, N. Keil, H. G. Bach, N. Grote, M. Spyropoulou, H. Avramopoulos, and Ch. Kouloumentas, "Tunable 100 Gbaud Transmitter Based on Hybrid Polymer-to-Polymer Integration for Flexible Optical Interconnects," J. Lightwave Technol. 34, 407-418 (2016)

[8] R. Oikawa, "A Feasibility Study on 100Gbps-Per-Channel Die-to-Die Signal Transmission on Silicon Interposer-Based 2.5-D LSI with a Passive Digital Equalizer," *2016 IEEE 66th Electronic Components and Technology Conference (ECTC)*, Las Vegas, NV, USA, 2016, pp. 957-965.

[9] A. Tatarczak, X. Lu, and I. Tafur Monroy, "Improving the Capacity of Short-Reach VCSEL-based MMF Optical Links," in *Latin America Optics and Photonics Conference*, (Optical Society of America, 2016), paper LTu3C.2.

[10] C. Yang *et al*., "IM/DD-Based 112-Gb/s/lambda PAM-4 Transmission Using 18-Gbps DML," in *IEEE Photonics Journal*, vol. 8, no. 3, pp. 1-7, June 2016.

[11] Kachris, Christoforos and Ioannis Tomkos. "A Survey on Optical Interconnects for Data Centers." *IEEE Communications Surveys and Tutorials* 14 (2012): 1021-1036.

[12] http://www.channelregister.co.uk/2009/11/27/ibm_power7_hpc_server/

[13] Selviah, D. R., Walker, A. C., Hutt, D. A., Wang, K., McCarthy, A., Fernández, F. A., Papakonstantinou, L., Baghsiahi, H., Suyal, H., Taghizadeh, M., Conway, P., Chappell, J., Zakariyah, S. S., Milward, D., Pitwon, R., Hopkins, K., Muggeridge, M., Rygate, J., Calver, J., Kandulski, W., Deshazer, D. J., Hueston, K., Ives, D. J., Ferguson, R., Harris, S., Hinde, G., Cole, M., White, H., Suyal, N., Rehman, H. u. and Bryson, C. "Integrated optical and electronic interconnect PCB manufacturing research"Circuit World, 36(2),pp. 5-19 (2010)

[14] Ingham, J. D., Bamiedakis, N., Penty, R. V., White, I. H., DeGroot, J. V. and Clapp, T. V. "Multimode Siloxane Polymer Waveguides for Robust High-Speed Interconnects" Proceedings of CLEO/QELS, pp. CThS4, (2006)

[15] Bamiedakis, N., Beals, J., Penty, R. V., White, I. H., DeGroot, J. V. and Clapp, T. V. "Low Loss and Low Crosstalk Multimode Polymer Waveguide Crossings for High-Speed Optical Interconnects" Proceedings of CLEO, pp. 1-2, (2007)

[16] A. La Porta, R. Dangel, D. Jubin, F. Horst, N. Meier, D. Chelladurai, B. Swatowski, A. Tomasik, K. Su, W. K. Weidner, and B. J. Offrein, "Optical Coupling between Polymer Waveguides and a Silicon Photonics Chip in the O-band," in*Optical Fiber Communication Conference*, OSA Technical Digest (online) (Optical Society of America, 2016), paper M2I.2.

[17] Kevin Kruse, Christopher Middlebrook, Laser-direct writing of single mode and multi-mode polymer step index waveguide structures for optical backplanes and interconnection assemblies, Photonics and Nanostructures - Fundamentals and Applications, Volume 13, January 2015, Pages 66-73, ISSN 1569-4410

[18] N. Keil, D. Felipe, Z. Zhang, M. Kleinert, C. Zawadzki, W. Brinker, A. Polatynski, G. Irmscher, M. Möhrle, H. Bach, and M. Schell, "Novel Integration Technologies for Disruptive Capacity Upgrade in Data Centre Systems," in *Optical Fiber Communication Conference*, OSA Technical Digest (online) (Optical Society of America, 2016), paper Th3F.3.

[19] R. Dangel, J. Hofrichter, F. Horst, D. Jubin, A. La Porta, N. Meier, I. Soganci, J. Weiss, and B. Offrein, "Polymer waveguides for electro-optical integration in data centers and high-performance computers," Opt. Express 23, 4736-4750 (2015)

[20] R. Dangel, C. Berger, R. Beyeler, L. Dellmann, M. Gm¨ur, R. Hamelin,F. Horst, T. Lamprecht, T. Morf, S. Oggioni,M. Spreafico, R. Stevens, andB. J. Offrein, “Polymer-waveguide-based board-level optical interconnect technology for datacom applications,” *IEEE Trans. Adv. Packag.*, vol. 31,no. 4, pp. 759–767, Nov. 2008.

[21] T. Lamprecht, et al.,” Highly Reliable Silicone Based Optical Waveguides Embedded in PCBs”, in OFC, OSA Technical Digest (online) (Optical Society of America, 2014), paper Th4J.5

[22] Brandon W. Swatowski ; Chad M. Amb ; Sarah K. Breed ; David J. Deshazer ; W. Ken Weidner ; Roger F. Dangel ; Norbert Meier ; Bert J. Offrein;

Flexible, stable, and easily processable optical silicones for low loss polymer waveguides. Proc. SPIE 8622, Organic Photonic Materials and Devices XV, 862205 (February 20, 2013);

[23] N. Bamiedakis, J. Beals, R. V. Penty, I. H. White, J. V. DeGroot and T. V. Clapp, "Cost-Effective Multimode Polymer Waveguides for High-Speed On-Board Optical Interconnects," in *IEEE Journal of Quantum Electronics*, vol. 45, no. 4, pp. 415-424, April 2009.

[24] Xingcun.T. (2014). Advanced Materials for Integrated Optical Waveguides. Springer International Publishing

[25] Hunsperger.R.G. (1984). Integrated Optics: Theory and Technology. New York. Springer-Verlag

[26] http://fibercore.com/fiberpaedia/attenuation

[27] Ghatak, Ajoy and K. Thyagarajan. An Introduction to Fiber Optics. 1st ed. Cambridge: Cambridge University Press, 1998. Cambridge Books Online. Web. 30 August 2016.

[28] Kevin Kruse, Karl Walczak, Nicholas Thomas, Brandon Swatowski, Casey Demars, Christopher Middlebrook, "Chemical inertness of UV-cured optical elastomers within the printed circuit board manufacturing process for embedded waveguide applications," Proc. SPIE 8988, Integrated Optics: Devices, Materials, and Technologies XVIII, 898811 (8 March 2014);

A Copyright Documentation

Figure 1: https://www.nextplatform.com/2016/11/14/closer-look-2016-top-500-supercomputer-rankings/. Accessed October 2017

Figure 2: The Power7 IH node hub/switch network. https://www.theregister.co.uk/2009/11/27/ibm_power7_hpc_server/?page=3. Accessed October 2017

Figure 4: Roger Dangel. Optical backplane of 192 channels with complex channel shuffling based on 8 stacked polymer waveguide flexes (after connectorization) https://www.osapublishing.org/oe/abstract.cfm?uri=oe-23-4-4736#figanchor3. Accessed October 2017

Figure 5: Roger Dangel. Optical transmitter card of a 12 × 10 Gbit/s optical-link demonstrator containing 12 embedded multi-mode polymer waveguides. https://www.osapublishing.org/oe/abstract.cfm?uri=oe-23-4-4736#figanchor3. Accessed October 2017

Figure 9: Propagation fiber optic.png. http://datacombyfloyd.blogspot.com/2010/07/fiber-optic-cables-and-nature-of-light.html. Accessed October 2017

Figure 10: 5728.jpg. https://www.fibercore.com/fiberpaedia/attenuation. Accessed October 2017